AN ABSTRACT OF THE THESIS OF

W. Scott Helms for the degree of Master of Science in Radiation Health Physics presented on November 24, 2014

Title: A Quantitative Comparison of Cardiovascular Imaging Systems With Respect to the Resolution Capabilities and the Resulting Skin Entrance Doses Operating in Both Fluoroscopic and Cine Mode

Abstract approved:

_____

Kathryn A. Higley

The increasing use of medical procedures using ionizing radiation has increased significantly in recent years. In 1987, the National Council on Radiation Protection Report 93 (NCRP) reported that the average exposure ionizing radiation was 53mRem/year (0.53mSv/year). In their most recent study on radiation exposures NCRP Report 160 in 2009, the average exposure to ionizing radiation was 297.6mRem/year (2.976mSv/year). This is increase of over 243.6mRem/year (2.436mSv/year).

In an effort to show that modern invasive cardiovascular imaging systems with their advanced imaging hardware and image reconstruction software processes; a reduction in the patient exposure rate while providing acceptable image resolution is

possible. Several imaging systems were tested using both image intensified (II) and flat panel detector (FPD) imaging.

By reducing the entrance exposure rate, diagnostic acceptable image spatial and contrast resolution standards were exceeded. The dose rate reduction from using a FPD over an II system in the same fluoroscopic normal dose mode of operation was over 10.2%. An even greater dose reduction of 38.8% was seen by operating the FPD in low fluoroscopic dose mode while maintaining diagnostic acceptable image spatial and contrast resolution standards as well. A similar reduction in dose rates were seen while operating in the cine mode of imaging.

A Quantitative Comparison of Cardiovascular Imaging Systems With Respect to the Resolution Capabilities and the Resulting Skin Entrance Doses Operating in Both Fluoroscopic and Cine Mode

by

W. Scott Helms

A THESIS

submitted to

Oregon State University

in partial fulfillment of

the requirements for the

degree of

Master of Science

Presented November 24, 2014

Commencement June 2015

Master of Science thesis of W. Scott Helms presented on November 24, 2014

APPROVED:

Major Professor representing Radiation Health Physics

Head of the Department of Nuclear Engineering & Radiation Health Physics

---

Dean of the Graduate School

I understand that my thesis will become part of the permanent collection of Oregon State University libraries. My signature below authorizes release of my thesis to any reader upon request.

W. Scott Helms. Author

TABLE OF CONTENTS

LIST OF FIGURES

Figure Page

LIST OF FIGURES (continued)

Figure Page

LIST OF FIGURES (continued)

Figure Page

LIST OF TABLES

LIST OF TABLES (continued)

LIST OF TABLES (continued)

Chapter1

OBJECTIVES

The objective of this exercise was to compare the spatial and low contrast imaging resolution capabilities of fluoroscopic imaging equipment using flat panel detectors with respect to the patient skin entrance exposure. A second objective was to determine if low dose modes of operation can produce clinically diagnosable images as defined by the current acceptable limits of the American Association of Physicists in Medicine (AAPM). A few older technology image intensified units were tested as well to show the advancement of the present technology as a comparison.

Chapter 2

BACKGROUND

2.1 Basics of Fluoroscopy

Fluoroscopy is an imaging technique commonly used by physicians to obtain real-time images of the internal structures of a patient through the use of a fluoroscope. In its simplest form, a fluoroscope consists of an x-ray source and a device to collect the x-ray photons emerging from the patient. In figure 2.1 a typical fluoroscopy imaging chain is shown.

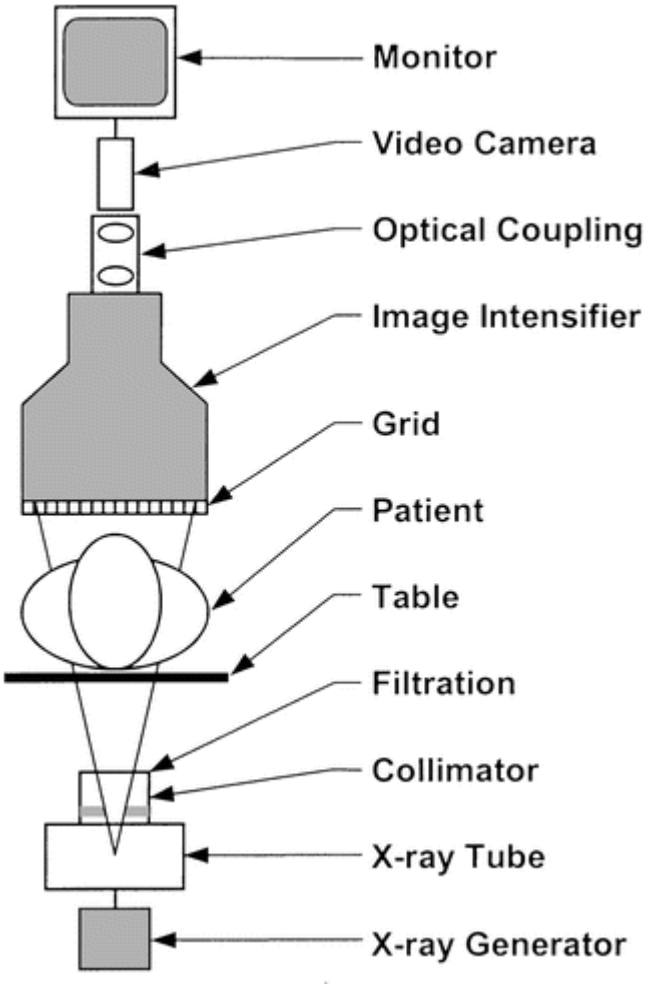

Figure 2.1. Typical Fluoroscopic imaging Chain[1].

The imaging chain starts with the X-Ray generator. The generator provides the large voltage and current to the x-ray tube. The generator also contains transformers to convert the incoming line voltage and current for specific circuits in the imaging chain. In addition to the circuit that provides the large peak voltage potential difference (kVp) between the anode and the cathode of the x-ray tube, there are circuits that control the tube mill-amperage (mA) current, as well as timers to control the length of time the electrons are allowed to flow to the x-ray anode from the cathode. The generator also provides energy to the circuits in the image intensifier (II) or flat panel detector (FPD) to control the automatic brightness control (ABC). Pulse rates and the ABC will be discussed in a later section of this report detailing the methods of patient exposure dose reduction.

After the generator, the next component of the fluoroscopic imaging chain is the x-ray tube. A typical x-ray tube with the basic components is shown in figure 2.2.

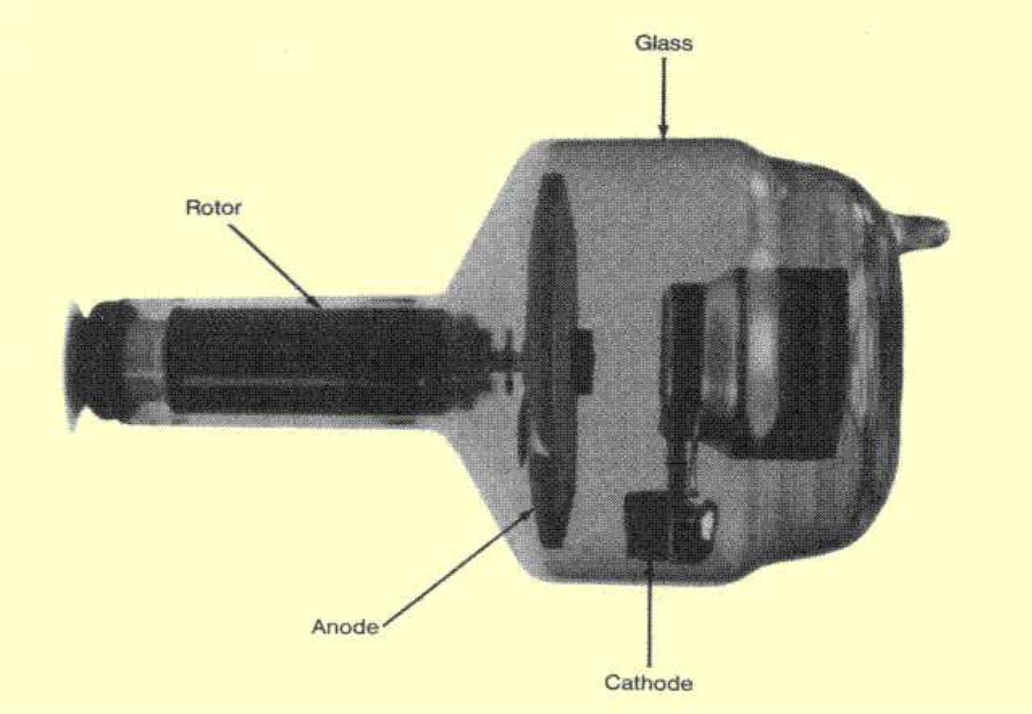

Figure 2.2. Typical X-Ray Tube with a rotating Anode[2].

The x-ray tube consist of a cathode, an anode, a motor to rotate the anode, oil to aid in cooling the tube, an evacuated glass housing to keep out air, a high tension cable to transmit the high voltage from the generator. The x-ray tube uses a large potential difference (kVp) between the cathode (the source of electrons) and the anode (the target) of the x-ray tube to create a driving force to increase the kinetic energy (KE) of the electrons. It does so by causing the electrons to travel from the negative charged cathode to the positive charged anode. The electrons are boiled off the filament by the current supplied by the generator by thermionic emission. The electrons are then accelerated toward the target where they interact with the target material, releasing their energy in the form of heat and x-rays. About 99% of the total electron energy is converted to heat leaving 1 percent available for x-ray production[3]. Both the filament and the anode are made from tungsten due to its high melting point and large atomic number (74). Due to the large amount of heat generated during x-ray production a rotating anode is used to dissipate the heat over the greater area of the anode. There are 2 modes of x-ray production occurring in the x-ray tube: characteristic and bremsstrahlung process. The production of characteristic x-rays occurs when a projectile electron interaction ejects a shell electron from the target atom. The ionized atom, now being in a higher energy state, will fill the inner shell vacancy with an outer shell electron. As a result, characteristic x-rays are released with energy equal to the difference in the binding energies (BE) between the two shells involved. For example, for a tungsten atom the binding energy (BE) of the K (inner) shell is 69.5keV, while the

BE of the L (next outer) shell is 10.2keV. A K - L shell transition would then release a 69.5keV - 10.2keV = 59.3keV x-ray. When the projectile electrons' KE is less than the binding energy of the target electron, excitation of the inner shell electron occurs and does not produce characteristic x-rays. Figure 2.3 depicts the sequence of events during characteristic x-ray production.

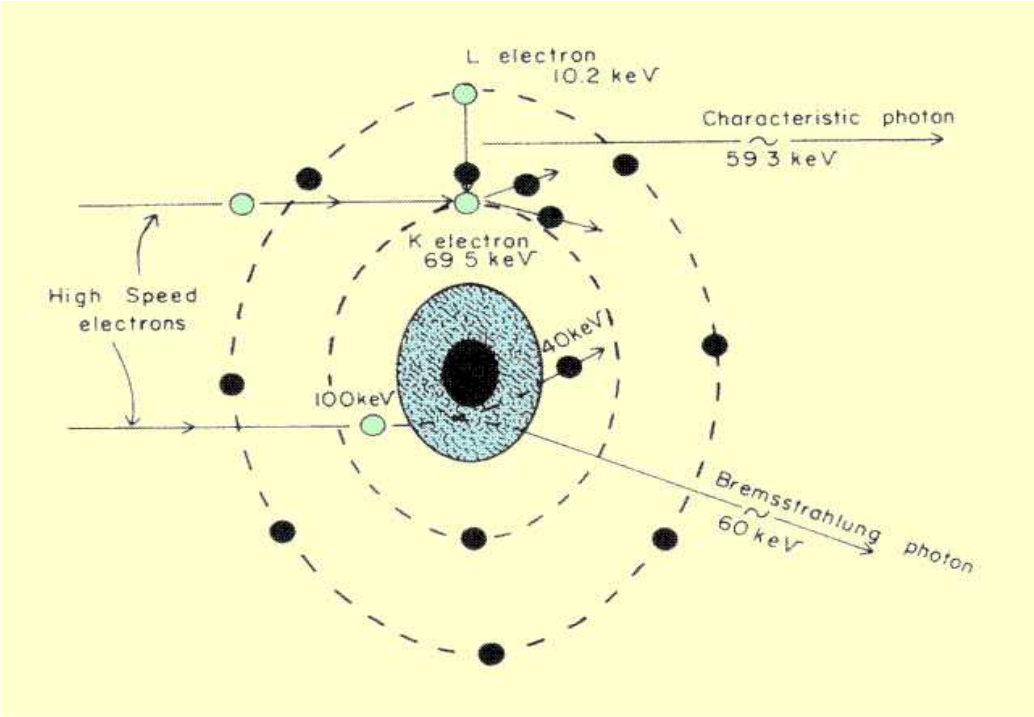

Figure 2.3. Characteristic and Bremsstrahlung X-Ray Production[2].

During the bremsstrahlung process, the accelerated electron comes in close proximity to the nucleus of the target material. Because of the coulombic attraction between the positive nucleus and the negative electron, the electron will decelerate or change direction, resulting in a loss of KE. This "lost" energy will then appear as

electromagnetic energy in the form of an x-ray. Figure 2.3 depicts bremsstrahlung x-ray production from a projectile electron with a energy of 100keV.

The amount of KE lost during the bremsstrahlung process depends on the proximity of the accelerated electron to the nucleus. As the electron – nucleus distance is decreased, the attractive coulombic forces between the nucleus and the electron causes the electron to alter its travel path to a greater extent. This change in the electron's travel path is a deceleration and the electron loses KE by emitting an x-ray. The maximum energy of an x-ray emitted from an x-ray tube occurs at the applied potential difference (kVp) that is selected by the automatic brightness control (ABC). The efficiency of bremsstrahlung production increases with increasing atomic number (Z) of the target or with increasing electron energy (kVp). Figure 2.4 shows a spectrum of x-ray energies from both characteristic and bremsstrahlung production processes. The x-ray tube in this example was operated at a potential difference of 80kVp.

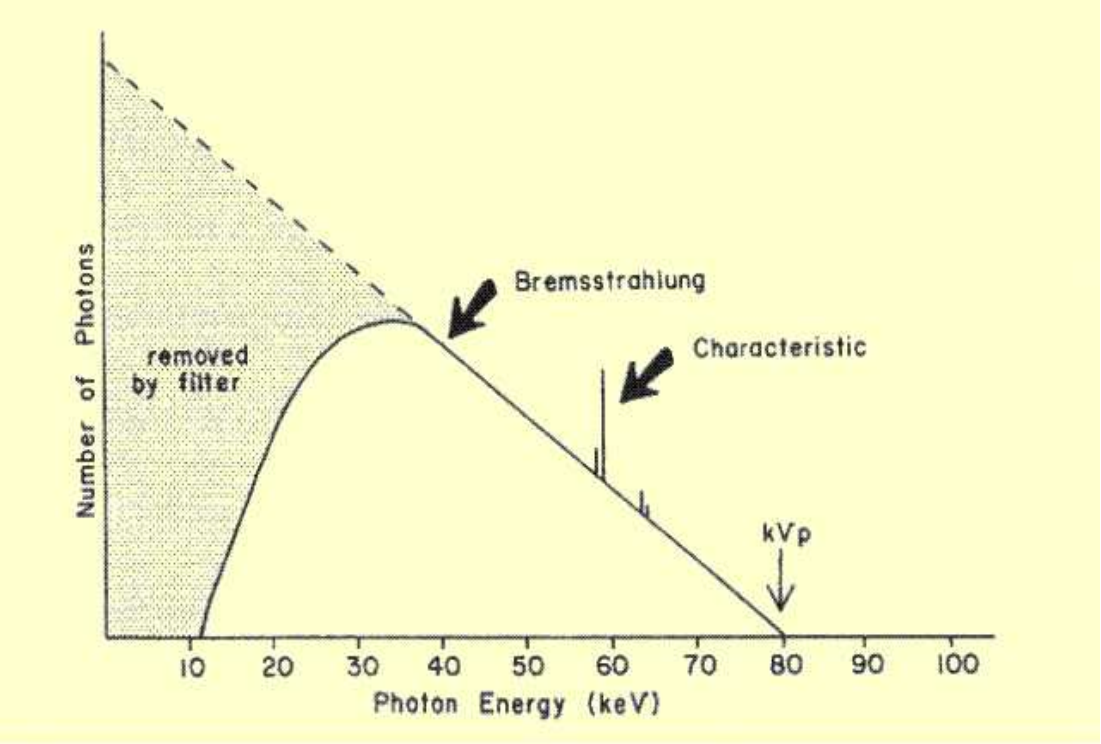

Figure 2.4, X-Ray Energy Spectrum of Characteristic and Bremsstrahlung X-Ray Production[2].

Between the x-ray tube and the collimators are aluminum filters which remove low energy x-rays. These low energy x-rays would only increase patient dose and not contribute to image formation. The gray shaded area in figure 2.4 depicts the low energy photons that are remove from the photon energy spectrum. The federal government has required standards to ensure the x-ray tube is operating with sufficient filtration as required by federal regulations under CFR Title 21 Part 1020.30.

The next component in the imaging chain is the collimators. The collimators act to limit the area of exposure of the useful x-ray beam. The collimators attenuate the x-ray beam by using blades made from a high atomic number material. By limiting the x-

ray beam, the area of exposed tissues is controlled and therefore helps reduce the patient's dose and also lowers the amount of scatter radiation that lowers the image contrast and lowers image quality. Additional spectral filters are placed in the collimator housing to shape the x-ray spectrum and effect image contrast and lower the patient dose by removing lower energy x-rays. These filters can be copper or aluminum and can vary in thickness.

The patient table is next in the imaging chain. The table has to be able to accommodate large patients without attenuating the useful x-ray beam that has emerged from the collimator. The table top material of choice is carbon fiber because of its low atomic number and good strength characteristics. At the energy levels used in medical imaging, the x-rays entering the patient can interact with the patient in one of three ways: Compton scattering, photoelectric effect, or no interaction at all. Compton scattering is an inelastic scattering process where the x-ray photon interacts with a material's electron resulting in the removal of the material's electron (Compton electron) from its orbital shell and the post collision photon scattered at an angle with a loss of energy and increased wavelength. Mathematically the energy transfer involved in Compton scattering interaction is defined as $E_{pi} = E_{ps} + (E_{be} + E_{ke})$ were E_{pi} is the energy of the initial photon, E_{ps} is the energy of the scattered photon, E_{be} is the binding energy required to remove a target material's orbital shell electron and E_{ke} is the kinetic energy of the projectile electron or Compton electron. A schematic of Compton scattering is shown in Figure 2.5.

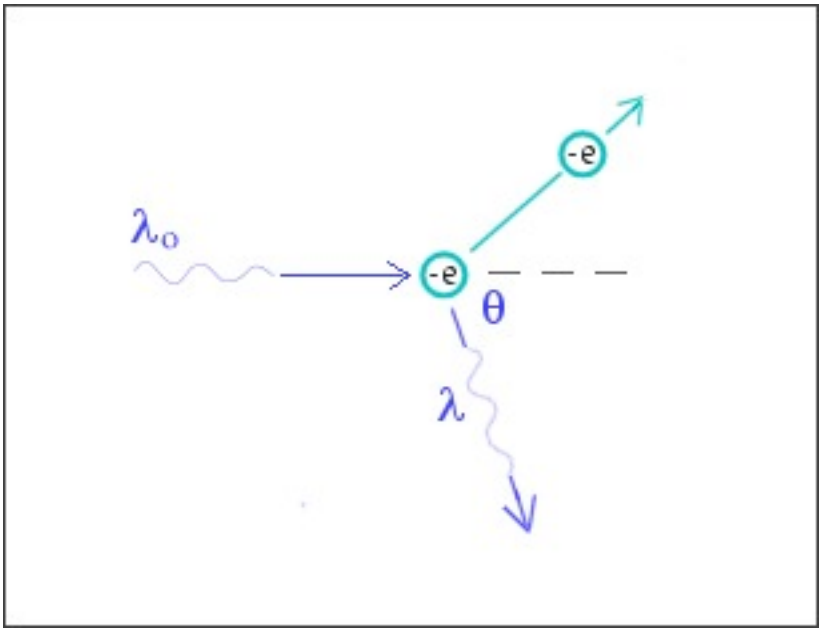

Figure 2.5. Compton scattering diagram[4].

Compton scattering can occur at all energies encountered in diagnostic radiology imaging. The probability of Compton scattering occurring is independent of the atomic number of the interacting material. Compton scattering serves to increase the radiation dose to the patient and affects image quality negatively because the x-ray photon's path of travel has changed with a lower KE that could be absorbed by the interacting material. The Compton electron loses its energy to the interacting material.

The photoelectric interaction occurs when an incident x-ray photon interacts with a bound electron of a target atom, with the photon's energy being total absorbed and the electron being removed from its shell. The dislodged electron is called a photoelectron and has KE equal to the difference of the BE of the electron and the x-ray photon. The target atom is left in an elevated energy state and releases a characteristic x-ray when an outer shell electron moves down to fill the inner shell vacancy. Mathematically the energy transfer involved in the photoelectric interaction is defined as

$E_{pe} = (E_{ke} - \varphi)$ were E_{pe} is the energy of the photoelectron, E_{ke} is kinetic energy of the x-ray photon and φ is the ionization potential of the interacting material. The ionization potential is the amount of energy required to remove the least bound electron in a material. A schematic of a photoelectric interaction is shown in Figure 2.6.

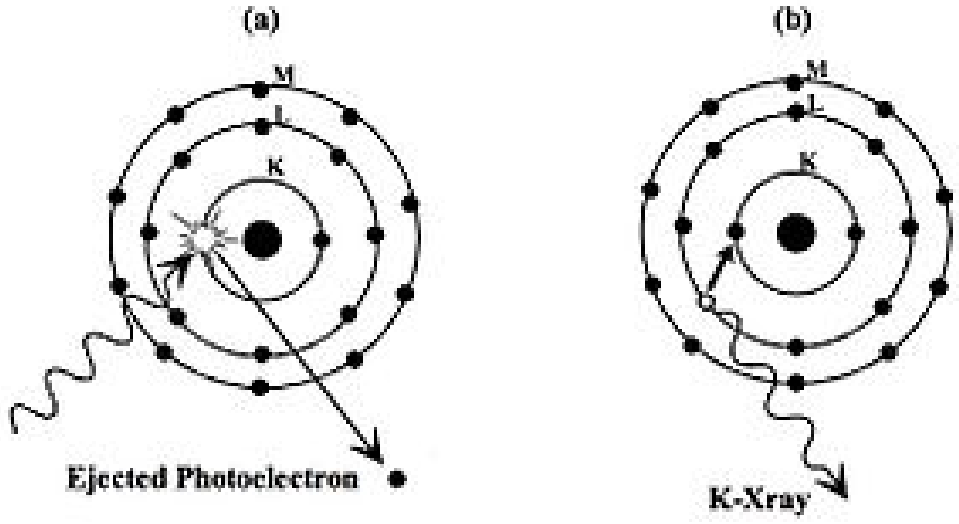

Figure 2.6. Photoelectric Interaction diagram[5].

The probability of a photoelectric interaction occurring is inversely proportional to the third power of the x-ray photon's energy and proportional to the third power of the target matter's atomic number. The characteristic x-ray emitted after a photoelectric interaction serves only to increase the radiation dose to the patient and does not increase the image quality because the photoelectric x-ray photon will most likely travel in a different direction than the original x-ray photon. Classical scattering interactions with matter occur with x-ray photon energies below 10keV and are absorbed by filters before interacting with the patient; pair production and photodisintegration interactions occur

with x-ray photon energies of 1.02MeV and above 10MeV respectfully and are well out of the useful photon energies used in diagnostic medical imaging.

Once the x-rays exit the patient, some of the photons in useful x-ray beam have been scattered out of their original path and no longer can contribute useful information in forming a medical image. These scattered x-rays need to be removed before they reach the imaging receptor whether it is the II or the FPD. The scattered x-rays will only lower the image contrast and decrease the sharpness of the image. The scattered x-ray photons can also serve as a source of radiation exposure to the individual standing next to the patient's side if the x-rays scatter at an angle and interact with them. A grid is placed in close proximity to the II or FPD to remove these unwanted x-rays from interacting with the image detector. However, the grid can also remove x-rays that were not scattered. So the output of x-rays from the x-ray tube is increased by the equipment's automatic brightness control (ABC) function to compensate for this decrease of photons which increases the dose to the patient. At this point the differences between II and FPD imaging chain's diverge. In the past, the fluoroscopy unit featured a fluorescent screen that was part of an image intensifier (II) and dates back to the 1960's. While this system is still used today in general fluoroscopy, (such as imaging of the gastroenterology tract) the current imaging systems found in cardiovascular imaging laboratories (CVL) use digital flat panel detectors (FPD) and have been in used in increasing clinical service since 2000.

2.2 Image Intensified Fluoroscopy

With respect to figure 2.7 (below) the sequence of events to produce a fluoroscopic image is as follows: x-ray photons exiting the anti-scatter grid (to remove image quality degrading scatter radiation) first encounter the input window, which is made from aluminum with its low atomic number, and therefore reduces the x-ray photon absorption and gives structural strength. The input window's aluminum thickness is generally about 1mm. After the input window, the x-rays impinge on the input phosphor (a cesium iodine compound screen) and are converted to light photons. This process is called luminescence.

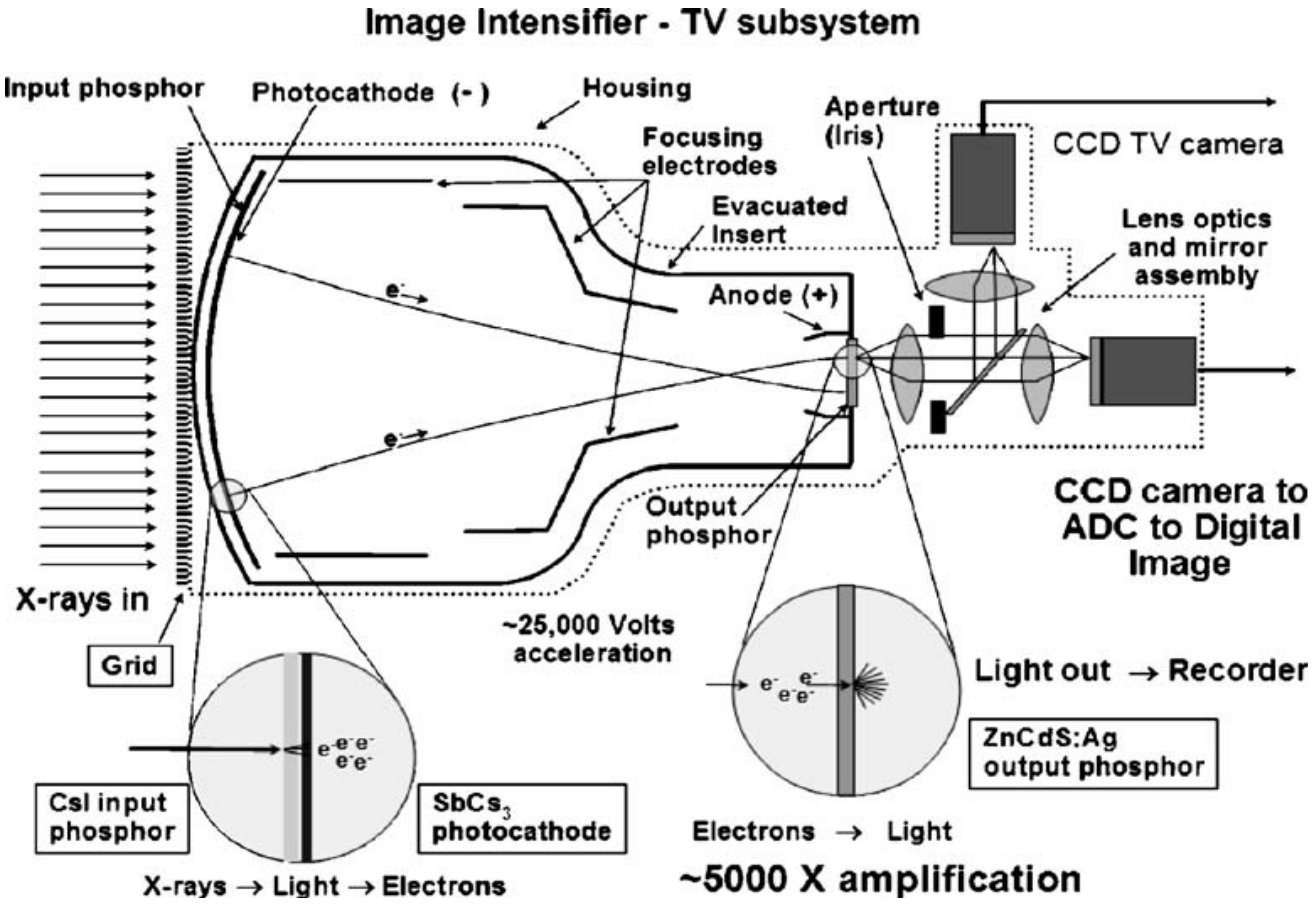

Figure 2.7. The Image Intensified Fluoroscopic Imaging Events[6]

Cesium iodide, (CsI) is used because of its increased absorption abilities (due to its high atomic number Cs = 57 and I = 53). Its mass attenuation coefficient best matches the energy spectrum of the energies of x-rays emitted from the patient (as shown in figure 2.8) when compared to other input phosphors. The mass attenuation coefficient describes the material's probability of interacting (Compton scattering and Photoelectric effect) with an x-ray photon with [respect to the materials density].

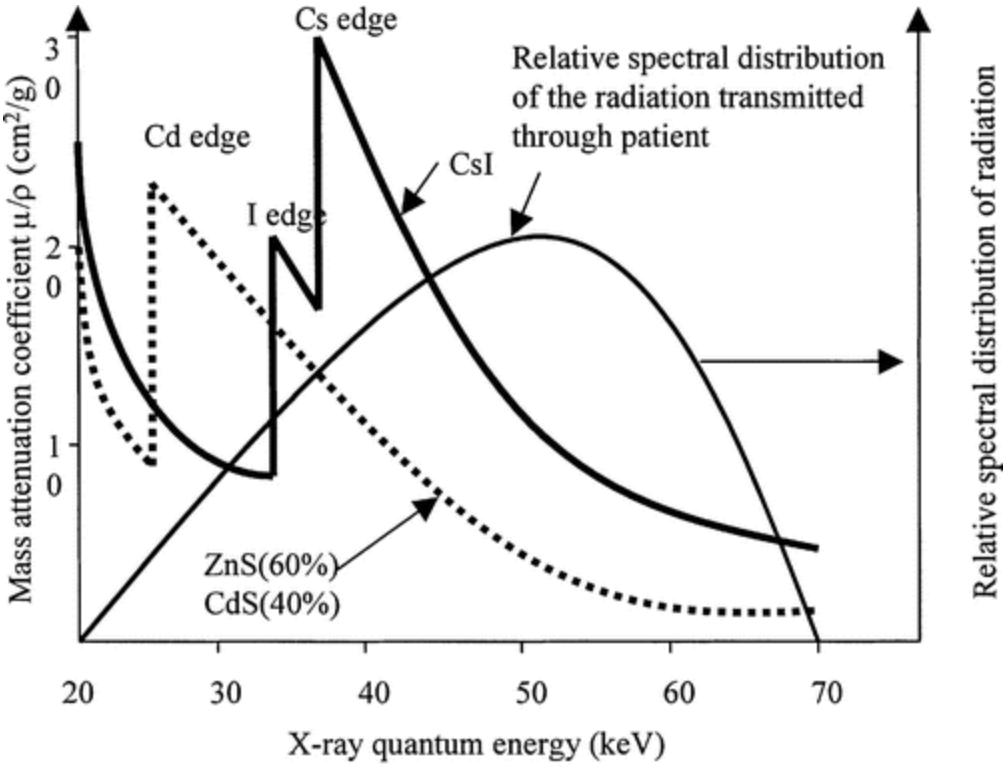

Figure 2.8. The spectral matching comparisons of input phosphor and photocathode materials[7]

The physical structure of CsI, with its needle shaped light pipes allows for better packing efficiency and therefore brighter light emission. The thickness of the CsI input

phosphor is roughly 300 to 450 um[6]. Because light intensity decreases with distance, the light is not observed directly but instead interacts with a photocathode constructed of an antimony cesium ($SbCs_3$) compound. The $SbCs_3$ compound has an absorption sensitivity that closely matches the light wavelengths that are emitted by the CsI input phosphor. The photocathode absorbs the light photons and in turn releases electrons (the photoelectric effect) that are focused by negatively charged electrodes and are driven toward a positive charged anode by a potential difference of 25 kVp between the photocathode and the anode enclosed evacuated glass insert. The electrons pass through an opening in the anode and interact with an output phosphor that is about 0.5 inches in diameter. The zinc cadmium output phosphor converts the electrons back to light photons and are transmitted to a charged couple device (CCD) television camera (solid state array of light sensors). The signal is converted to a digital signal by an analog-to-digital converter for image viewing and image recording devices. The converted electronic signal adds electronic noise to the image. The image viewing monitors used in this exercise were liquid crystal display (LCD).

Magnification of the image (decreasing the field of view (FoV)) as seen on the image monitor is achieved increasing the charge on the focusing electrodes and collimating the useful x-ray beam exiting the x-ray tube. In a larger II diameter, the entire input phosphor is used to produce the image. As an example, say the input phosphor has a diameter of 25 cm. As a smaller size is used (17cm), the charge on the focusing electrodes is increased thus causing the focal point to move further from the output phosphor. The end result is a magnified image that is in direct proportion to the ratio of the diameters. The 25 to17 cm example listed above would produce a magnified image

1.5 times larger than the image in the 25 cm mode. However there is an important trade off to be made when going to a smaller FoV. When in the magnification mode, the minification gain (the ratio of the square of the diameter of the input phosphor to the square of the diameter of the output phosphor) is reduced thereby producing a dimmer image because the useful diameter of the input phosphor decreased while the output phosphor diameter remained constant. To compensate for the decrease in light being produced, the fluoroscopic x-ray tube, as controlled by the ABC, increases the tube's current in units of milli-amperage (mA, an increase in the number of electrons interacting with the x-ray tube's target making more x-rays) will be automatically increased thus giving the patient a larger exposure to ionizing radiation in the effort to create more light photons from the input phosphor.

2.3 Digital (Flat Panel Detector)(FPD)Fluoroscopy

As compared with the conventional II fluoroscopic imaging sequence, the FPD has a vastly different set of steps to image formation with respect to the sequence of events that occur. There are two methods in use today namely direct and indirect conversion image formation. The most prevalent method used in CVL imaging is indirect conversion. Figure 2.9 shows a cut away of a flat panel detector using indirect conversion image formation. Figures 2.10 and .2.11 are used to briefly summarize the two methods.

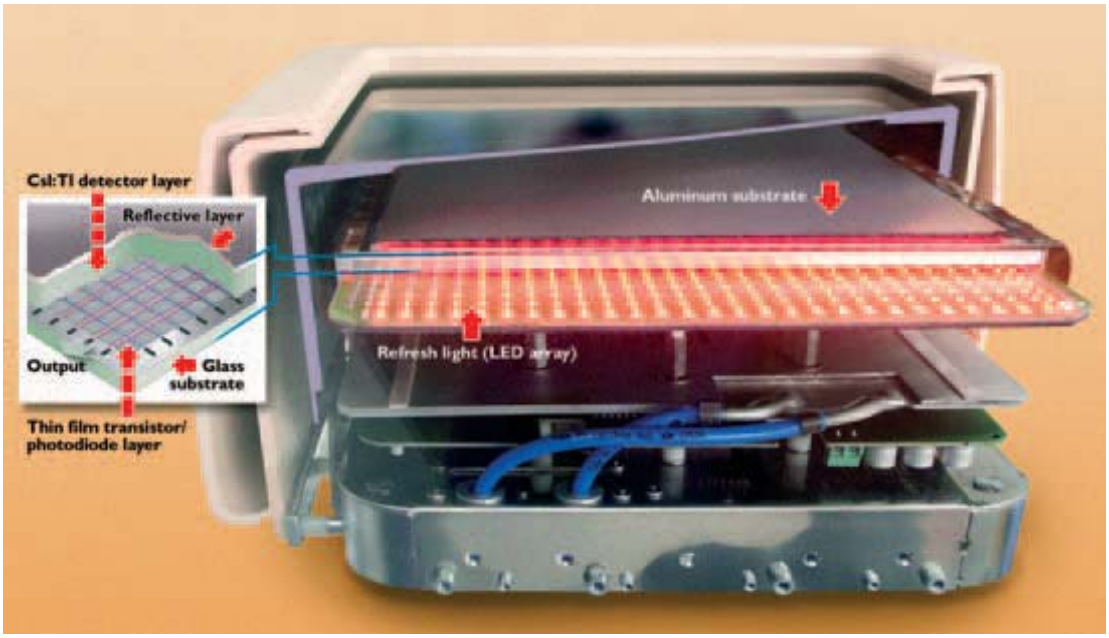

Figure 2.9. The Typical Flat Panel Detector[6] (TFT).

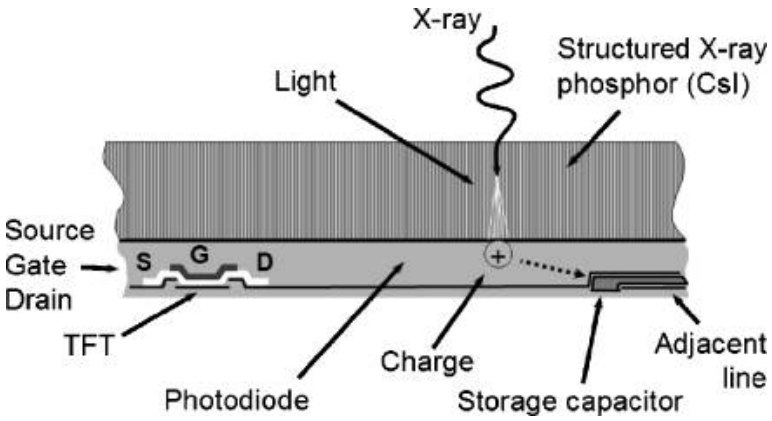

Figure 2.10. A Cross-section of an indirect TFT detector using Cesium Iodide structured phosphor shows the conversion of X-rays first into light, traveling through the structured phosphor to a photodiode etched on the TFT array and the creation of a proportional charge stored in the local capacitor[8].

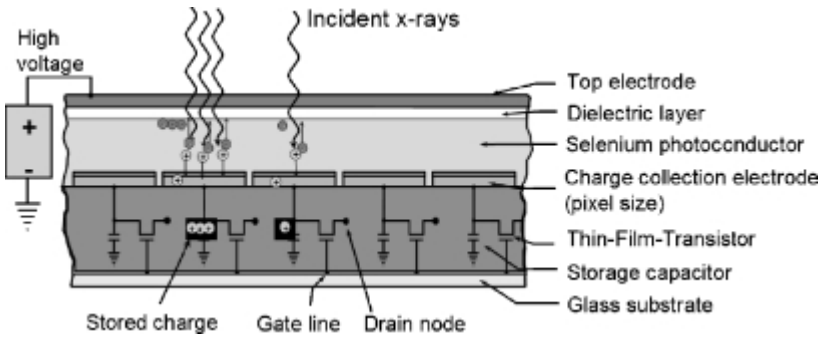

Figure 2.11. A Cross-section of a direct conversion TFT detector using a thick a-Se semiconductor layer under high voltage shows the creation of ion pairs directly by X-ray absorption, the separation and collection of the opposite charges at the electrodes, and the storage of the charge in the local capacitors[8].

Because this exercise only involved CVL units that used image intensifiers or flat panel detectors that use the indirect conversion method of image formation, this will end the discussion of direct conversion image formation.

Like the conventional II imagining system, an indirect conversion FPD uses an input phosphor (Cesium Iodide, CsI) material that absorbs the impinging X-rays and produces light photons. For II imaging systems, to achieve good x-ray absorption efficiency requires a thick phosphor, while acceptable spatial resolution requires a thin phosphor to reduce the scattering of the light photons. A compromise between the two concerns is made due to the curved surface on the input side of the II. This is not as great a concern for FPD imaging systems. The ability to use a thicker input phosphor on a flat geometric configuration is the main reason why FPD's achieve a higher absorption efficiency and are more efficient at converting x-rays into an image, thereby reducing the patient's exposure to ionizing radiation[10]. The typical input phosphor thickness for a

FPD is 550μm[6] as compared to the II input phosphor thickness of 300 to 450 um. Just as with an II based CVL units, the intensity of the x-ray beam is directly proportional to the intensity of the light produced by the input phosphor. The wavelength of the light emitted by the phosphor must match the photodiodes light absorption abilities. The peak light output wave length of CsI is 550nm and the amorphous silicon photodiode's peak light absorption efficiency is also at a wavelength of 550nm[11].

Once the light photon is absorbed by the amorphous silicon photodiodes (photocathode) and releases an electron (the photoelectric effect) to subsequently interact on a thin film transistor (TFT) array (flat panel X-ray imagers are based on solid-state integrated circuit (IC) technology, similar in many ways to the imaging chips used in digital photography and video[12]), to produce a corresponding charge in the detector element capacitor. The basic architecture of a-Si TFT device is arranged as a row and column array of detector elements as shown in figure 2.12

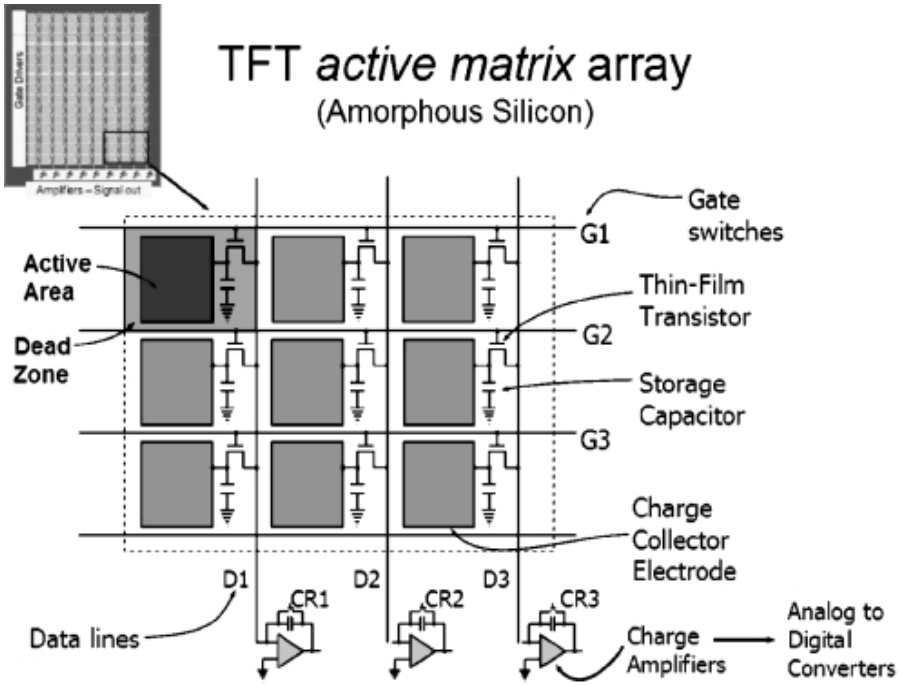

Figure 2.12. A TFT matrix array[8].

The TFT active matrix array is composed of millions of individual detector elements[8], each of which contains a transistor, charge collector electrode and storage capacitor, all arranged on an amorphous silicon substrate. Individual elements are connected by gate lines along rows (operating the TFT), by drain lines along columns (connected to the TFT output), and charge amplifiers connected to the drain lines to receive the charge signal from specific detector elements. The photodiode has five steps in its operation and is summarized below and shown schematically in figure 2.13. First each detector element in the array's capacitor is charged with an initial charge with the switches closed to complete the circuit. The switch is opened in step 2, but because there is no light emitted from the CsI input phosphor onto the surface of the detector element, the initial charge in the capacitor remains. In the third step, with x-rays impinge on the input phosphor, light is emitted and impacts on the detector element. The light

impacting the detector element causes the photodiode to conduct a current that is proportional to the intensity of the light emitted which is proportional to the x-rays absorbed by the input phosphor. As more light is emitted, more charge is removed from the capacitor. With step 4, the exposure is finished; the capacitor is left with a charge less than the initial charge that was placed on the capacitor. The final step concludes with a switch being closed and the remnant charge left in the capacitor actively read by turning row gate lines on one at a time, allowing charge to pass from the local storage capacitor through the TFT, down the drain line to the charge amplifier. Once the amplified signal is passed from the charge amplifier to the analog to digital converter, the digital signal is sent to a computer where imaging algorithms create the image. Another difference between II and FPD fluoroscopy units is that FPD imaging does not require a television camera to produce an electronic image and therefore there is a reduction in electronic noise which degrades the image. This electronic noise is independent of the quantum mottle image noise and increasing the number of x-ray photons will only make the electronic noise more apparent.

To prevent any residue charge from remaining in the capacitors, a refresh light (an LED array) is illuminated to remove any residue charge in the elements after each frame. A residue charge in an element will lead to an image artifact known as ghosting and reduce the image quality. Once the electronic signal is read from the detector array, the signal is sent to an analog to digital converter and the digital signal is then sent to an image viewing monitor and image recording devices. The image viewing monitors used in this exercise were liquid crystal display (LCD).

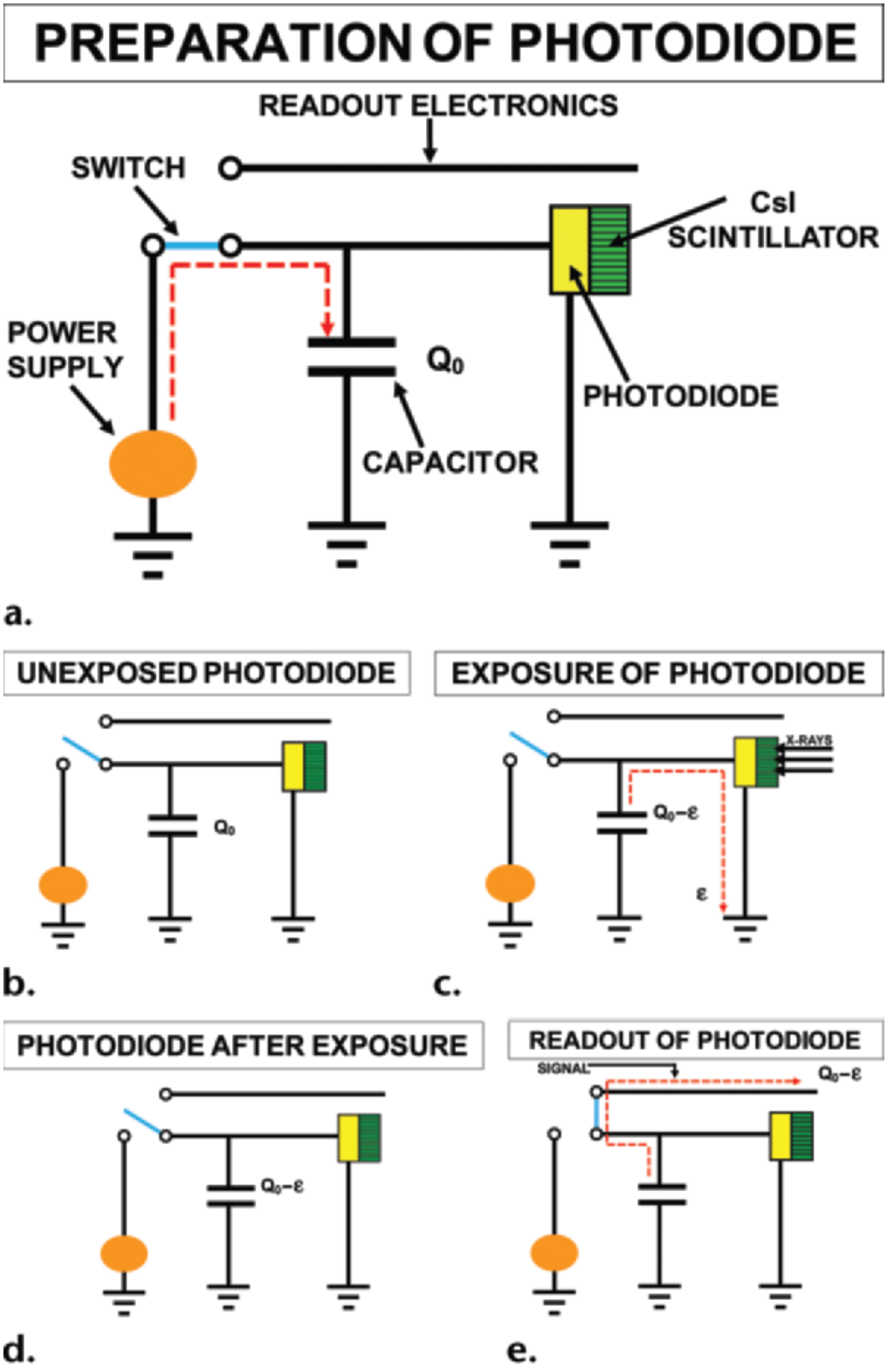

Figure 2.13. The photodiode five steps of operation[9].

Magnification of the FPD image is accomplished by one of two modes: 1). electronically zoom image, however there is no actual increase in the image resolution and is similar to zooming in a digital picture. 2). Detector element un-binning (if binning is allowed). With detector un-binning there is an increase in the spatial resolution. For digital flat panel fluoroscopy, how magnification affects a patient's exposure to radiation is complicated. If magnification un-bins pixels, then the dose increases to maintain the same SNR per pixel. If magnification is actually an electronic magnification with no actual increase in resolution, the patient dose will increase because both the unmagnified and magnified image will have same the SNR but the apparent noise (noise/mm^2 as viewed on monitor) will increase, and to overcome the increased noise level. The dose to the detector must increase, thereby increasing the dose to the patient[10].

Detector element binning is basically the coupling of adjacent detector elements by combining their readout signals, and is a way to improve image sensor video performance (temporal resolution) by reducing the data rate (MB/sec) read out. As an example of the amount of data to be collected and processed, a 40 × 40-cm FPD system may produce an image composed of 4 million detector elements, an image size of 8 MB, and a data rate as high as 240 MB/sec. Large data rates such as these are difficult for electronic systems to handle. Grouping four detector elements together reduces the data rate by 25% of the ungrouped rate for large field of views[9]. This method combines data signals from nearby sensor photo-sites prior to analog-to-digital conversion and read-out. By combining the charge prior to read-out, the signal is increased, the read-out noise is reduced and the analog to digital conversion rate is

increased. Further, the output channel rate is decreased. Pixel binning improves low light sensitivity and high speed video capture in exchange for image spatial resolution. Recall that the latent image as recorded in the pixels of the detector is in the form of an electrical charge collected and that each line of data is read sequentially. Therefore the detector cannot acquire another image until all data is read out (this is called dead time of the detector). The time needed to read the stored data is part of the reason for the need to bin pixels for faster frame rates that are required in cardiac imaging procedures. By combining two rows of pixels into one and readout as a single line of data, the reading of the super pixel is increased allowing for higher imaging rates. Binning pixels also results in less noise as the signal to noise ratio (SNR) is increased. For real-time fluoroscopic imaging, the readout procedure must occur fast enough to acquire data from all detector elements and occurs over a period of 33 ms or 30 frames per second[7].

2.4 Terms to Describe Image Quality and Equipment Operation

Contrast resolution

Contrast resolution describes the ability to distinguish between differences in attenuation/intensity in an image. Contrast resolution is used in medical imaging to determine the quality of acquired images and incorporate use factors encountered when imaging a test object. These factors include the x-ray energy spectrums that the automatic brightness control used by varying the potential difference in the x-ray tube, scatter radiation from the test phantom, and electronic noise. It is important when small contrast differences are required to diagnose pathologies. In this report the contrast

resolution is described as percent (%) contrast which is the difference in x-ray beam attenuation between an object and its surrounding medium. As the attenuation difference between the object and the surrounding medium decreases, the test objects become increasingly difficult to visualize. The AAPM with Report number 70, has suggested the contrast resolution limit of less than 2% for all FoV's during digital cine and less than 2.5% in any provided fluoroscopy mode. Unfortunately, the various criteria used by different observers for contrast detection can result in scoring variations.

Spatial resolution

Spatial resolution describes the detail an image contains. The term applies to digital images, film images, and other types of images. Higher resolution means more image detail. It is the ability to see spatial detail without blurring close structures into one structure, or how close lines can be to each other and still be visibly resolved. Spatial resolution can be measured in various ways. Resolution units are tied to physical sizes as lines per mm, lines per inch). As an example, a resolution of 10 lines per millimeter means 5 dark lines alternating with 5 light lines, or 5 line pairs per millimeter (5 LP/mm).

For image intensifying fluoroscopic systems using television monitors, the spatial resolution is defined by two (2) components: vertical and horizontal resolution. Vertical resolution depends on the number of rows of raster lines the image monitors. As the number of raster lines increases, the vertical resolution increases as well. For imaging

units using LCD monitors, rows of pixel elements in a matrix array replace the raster lines.

The horizontal resolution is defined by the bandwidth (the speed of the electronic readout). As the bandwidth increases, the horizontal resolution increases as well. While in the fluoroscopic imaging mode, the amount of information in the data signal is able to be transferred to the imaging monitor well within the timeframe of the acquiring frames per second. The resulting spatial resolution does not suffer due to the bandwidth at which the system operates. This is not the case while the system is operated in cine mode. In cine mode, the images recorded must be able to stand alone on their image quality without reference to a previous image and provide clinically diagnostic information. For this to be possible, higher dose rates to the patient, and therefore increased dose rates to the image detector are used to create a recorded “cine” image. This translates into more information being sent in the electronic signal. The bandwidth can only handle a specific amount of information before it has to compress the signal’s information by interpolating the signal, which causes the signal to lose some of its sharp shape and results in a loss of spatial resolution. FPD imaging systems units are also limited by the vertical and horizontal spatial resolution components in their spatial resolution capabilities. The electronic signal is sent from the image processing computer to the image monitor at a given bandwidth.

When viewing the images and describing both the percent contrast difference and spatial resolution patterns, one needs to be aware of the viewing conditions such as ambient lighting, distance from the image monitor and the monitor’s window width and

window leveling. To be consistent, ambient lighting was kept to a minimum. A greater observer to monitor distance was used for interpretation of the percent contrast difference grading while a closer distance was used for grading spatial resolution. The programmed or default window leveling settings were used as well.

Temporal Resolution

Temporal resolution describes the ability to resolve events at different points in time. An example of this is the imaging of a beating heart or the advancing of a catheter in a blood vessel with little or no blurring. The temporal resolution can be improved by limiting the pulse width of the x-ray tube. The pulse width is the time the electrons are allowed to flow from the cathode to the anode in the x-ray tube. Both fluoroscopy and cine imaging use pulse widths around 5 milliseconds.

Detector Quantum Efficiency

(DQE) describes how effective an x-ray imaging system can produce an image with a high signal-to-noise ratio (signal-to-noise ratio can be described as the ratio of useful information to irrelevant information) relative to an ideal detector. It describes the sensitivity of an x-ray receptor. DQE is defined as the ratio of the squared output signal-to-noise ratio $(SNR_o)^2$ to the squared input signal-to-noise ratio $(SNR_i)^2$. The DQE is dependent on the radiation exposure, spatial frequency, and the detector material[11]. The detector material is important because its linear attenuation coefficient and thickness describe how well it attenuates the x-ray photon beam.

The attenuation of an x-ray photon in the receptor is given by the equation: $N = N_o(e^{-\mu x})$ where N_o is the initial number of x-ray photons incident on the surface of the detector, N is the number of photons transmitted through the detector, μ is the linear attenuation coefficient and x is the thickness of the receptor/input phosphor. As x and μ increase, the ratio N/N_o goes to 0 (N goes to 0). This is the reason manufacturers try and increase the thickness of the CsI phosphor to its most efficient size.

At high dose rates typical of cine acquisition, the FPD DQE is better than the II. At low dose rates, typical of fluoroscopy mode, II and FPD show similar DQE[12]

Fluoroscopic Acquisition Rate Techniques

Rates of acquisition can also be set for each operator's personal preference or examination requirements. The acquisition rate is set to allow an image run that is pleasing to the operator's vision. if the rate is set to low, image flicker will occur. Since the temporal response of the human visual system has a typical integration time of approximately 0.1 s (up to 0.2 s for low light levels), it has the capacity to integrate several frames of pulsed fluoroscopy during a single integration cycle[13]. Fluoroscopy rates of acquisition range from a low of 3 pulses per second (PPS) to 30 PPS for FPD systems, and 3 PPS to a continuous rate for II based systems. As the pulse rate decreases, the exposure rate to the patient decreases as well.

Entrance Exposure Rate (EER) (R/min)

EER is the exposure rate measured in air at the point where the x-ray photons enter the body. In a C-arm type of fluoroscopy, the EER is measured 30 centimeters

from the input surface of the fluoroscopic imaging assembly. With the normal mode (non-high level), the maximum EER is set at 10R/min. While operating in high level or boost mode the EER limit is 20R/min.These limits are set by the Food and Drug Administration (FDA) CFR Title 21 Part 1020.32. X-ray photons are progressively absorbed as they pass through the body. For every 4 cm of tissue, the beam strength is reduced by about one-half. As a result, the dose received where the beam enters the body is much higher than the dose where it exits[14].

Detector Entrance Exposure Rate (DEER) (μR/sec)

The detector entrance exposure rate measures the effective “speed” of the imaging system, that is, the amount of radiation used in image formation[15]. Unlike the EER, there are no regulations limiting the detector entrance exposure rates. The DEER is used to evaluate the functionality of automatic brightness control circuit. Because this exercise involves comparing the patient entrance exposure rate with the resolution capabilities of a fluoroscopic imaging system, this subject will not be discussed further.

Automatic Brightness Control (ABC)

The ABC system controls the EER to the patient and the DEER to the II or FPD. It functions to prevent the fluctuation in image brightness and SNR that would make diagnosis or navigation of instruments difficult under fluoroscopic imaging. Fluoroscopic AEC may use the signal from a sensor such as a photodiode or a photomultiplier tube or, more commonly, the signal from the video camera or directly from a flat panel image receptor, to determine necessary adjustments of fluoroscopic technique factors such as

tube voltage and tube current[13]. When required, the ABC can make changes to the operating tube potential (kVp) or the operating tube current (mA) or change both the kVp and mA.

The ABC circuit continuously monitors the signal from sensor for changes in the signal. As an example if the operator of the fluoroscope navigates an object that has different mass attenuation coefficients within the volume of material being examined, upon going from a less to more dense material volume, the voltage comparator will detect that a decreasing change in voltage from the photomultiplier amplifier has occurred. A signal will be sent to the “kVp-control module” to increase the tube potential by 10 kVp. (If the current remained the same) The “mA-control module” receives a signal from the “kVp-control Module”, and will increase the tube current in accordance to a preprogrammed value based on the “fluoroscopy loading curve”**.** As the x-ray tube current rises, the required increase in tube potential is reduced to perhaps 5 kVp, rather than 10 kVp. This whole process may take about 2 seconds to achieve a new steady state of operation[16]. For this exercise, all of the tested imaging units had correctly functioning ABC controls.

Dose Modes

There are a few dose modes of operation that the fluoroscopy unit can operate and are based on altering the sensitivity of the image detector. There is usually a low, normal and high/boost dose mode. Different manufactures have different terms to describe these three setting. There are a few ways the exposure dose rate is lowered. One way low dose mode of operation is achieved is by added cooper filtration in the

radiation beam which “hardens” the beam, removing the low energy dose increasing x-ray photons. Some units add as much as 0.9 mm of cooper for the low dose mode and add 0.3 mm of cooper for the normal dose mode. By hardening the x-ray beam, the low contrast resolution scoring can suffer as the x-rays penetrate the phantom’s different contrast disks to a greater extent and reduce the ability to see subtle changes in contrast differences. Another way of achieving a low dose rate is by adjusting the sensitivity of the detector allowing the x-ray tube to operate at a lower tube current (mA) while maintaining the same kVp using special image processing algorithm techniques to smooth out the image noise levels by separating moving and non-moving object in the radiation field. The non-moving objects can be included from image frame to image frame thus reducing the noise level significantly.

2.5 Image Artifacts in Image Intensified Fluoroscopy

None of the units with image intensifier tubes involved in this exercise displayed any of the listed possible artifacts.

Lag

Lag is the persistence of luminescence after x-ray stimulation has been terminated. Lag degrades the temporal resolution of the dynamic image[8].

Vignetting

A fall-off in brightness at the periphery of an image is called vignetting. Vignetting is caused by the unequal collection of light at the center of the image intensifier

compared with the light at its periphery. As a result, the center of an image intensifier has better resolution, increased brightness, and less distortion[8].

Veiling Glare

Scattering of light and the defocusing of photoelectrons within the image intensifier are called veiling glare. Veiling glare degrades object contrast at the output phosphor of the image intensifier[8].

Pincushion Distortion

Pincushion distortion is a geometric, nonlinear magnification across the image. The magnification difference at the periphery of the image results from the projection of the x-ray beam onto a curved input surface. The distortion is easily visualized by imaging a rectangular grid with the fluoroscope[8].

S Distortion

Electrons within the image intensifier move in paths along designated lines of flux. External electromagnetic sources affect electron paths at the perimeter of the image intensifier more so than those nearer the center. This characteristic causes the image in a fluoroscopic system to distort with an S shape. Larger image intensifiers are more sensitive to the electromagnetic fields that cause this distortion. Manufacturers include a highly conductive mu-metal shield that lines the canister in which the vacuum bottle is positioned to reduce the effect of S distortion[8].

Defocusing

Electrons within the image intensifier are focused to the focal spot by negatively charged plates positioned in the image intensifier. If the charge on these plates begins to drift, the electrons will not impinge on the focal spot which will cause the image seen on the viewing monitor to be blurred.

2.6 Image Artifacts in Flat Panel Fluoroscopy

None of the units with flat panel detectors involved in this exercise displayed any possible artifacts.

All large area digital detectors have defects that results in artifacts and result in image raw data that is unsuitable for clinical display and there are multiple causes for these artifacts. Clusters of adjacent pixels can have different sensitivities to the radiation it is absorbing (gain factors). Pixels can be unresponsive (dead/burned out), There can also be data line drop off where the signal is lost and not transferred[10]. These artifacts can be corrected by computer software through interpolation techniques similar to CT image reconstruction. Ghosting is artifact that looks like phosphor burn in an image monitor; it is caused by not removing the residue charge in the TFT circuit.

Chapter 3

METHODS AND MATERIALS

The methods used in collecting the resolution data and patient EER were consistent with standards set by the American Association of Physicists in Medicine[17] (AAPM) and are listed below.

3.1 Entrance Exposure Rate (EER)

The entrance exposure rate including backscatter for a “typical” patient should be evaluated at least annually. In some regulatory environments, more frequent (i.e., quarterly or monthly) evaluation may be required. This measurement requires the system to be set up in the same geometric configuration as it is used for typical patient examinations, using automatic brightness control mode. This usually involves placing varying thicknesses of PMMA (polymethylmethacrylate or “acrylic”) or another tissue-mimicking attenuator (10, 20, and 30 cm thicknesses are recommended) in the radiation beam, and measuring the exposure between the x-ray tube and the entrance of the PMMA. The Automatic Brightness Control (ABC) system should be activated, and operated in a typical clinical mode. The EER should be made in all available magnification modes. A radio translucent dosimeter is required for these measurements to avoid interference with the ABC system. The ionization chamber should be placed at 30 cm in front of the input to the imaging assembly for entrance exposure rates

including backscatter. Figure 3.1 shows stacked acrylic plates on a patient couch to measure the EER.

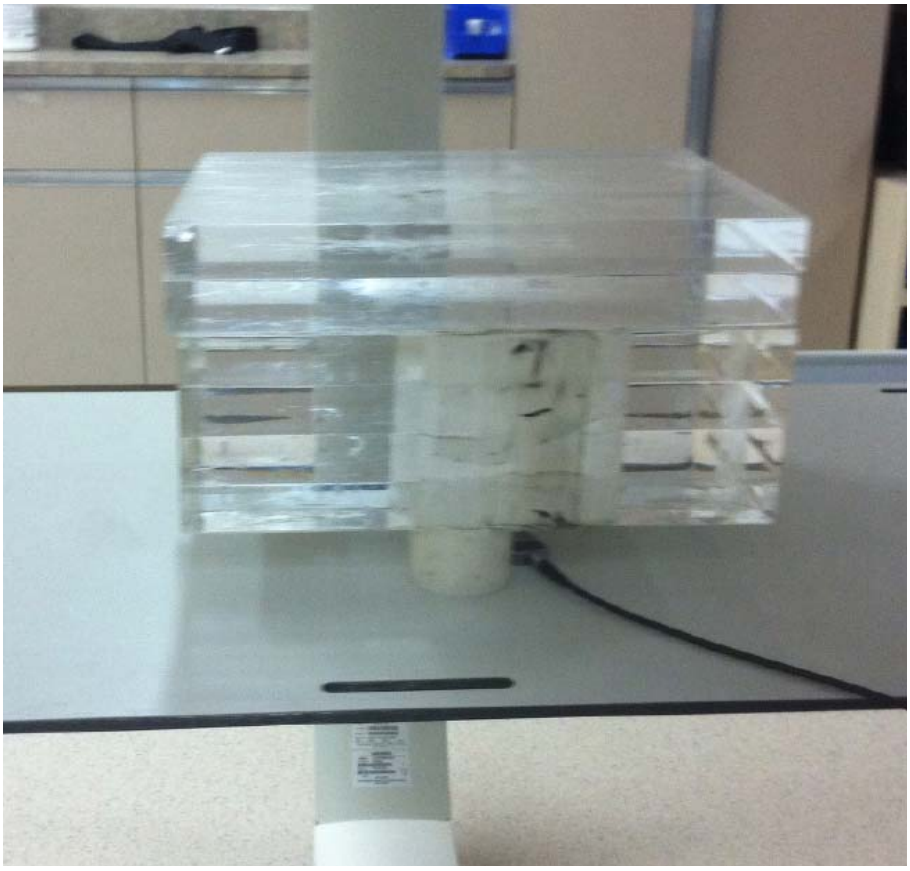

Figure 3.1. Entrance Exposure Rate Experimental set up showing 6 1” Acrylic plates with the radiation detector 30cm from the fluoroscopic detector input area.

3.2 Spatial Resolution.

Spatial resolution of the system should be determined by taping a line pair phantom to the center of the front surface of the II/FPD. A Nuclear Associates model # 07-532-2 line pair phantom was used in this exercise. The line pair phantom is to be positioned 45 degrees with respect to the video scan lines and grid lines. Typically, a line pair phantom with the range of 0.7 to 5.0 line pairs/mm is used. Only the resolution tool was placed in the radiation beam, the line pair corresponding to the highest spatial frequency that is visible under ABC-controlled fluoroscopy was recorded. Both theoretical and achievable measured spatial resolution values have been published. It is important that the same individual be responsible for this test from time to time, to reduce the degree of subjective error. As stated in the previous section, little ambient light was used to score the resolution of each fluoroscopic unit. If multiple television monitors existed, the one used most by the imaging physician during fluoroscopic studies was used to make the measurement. Figure 3.2 shows the spatial resolution test phantom.

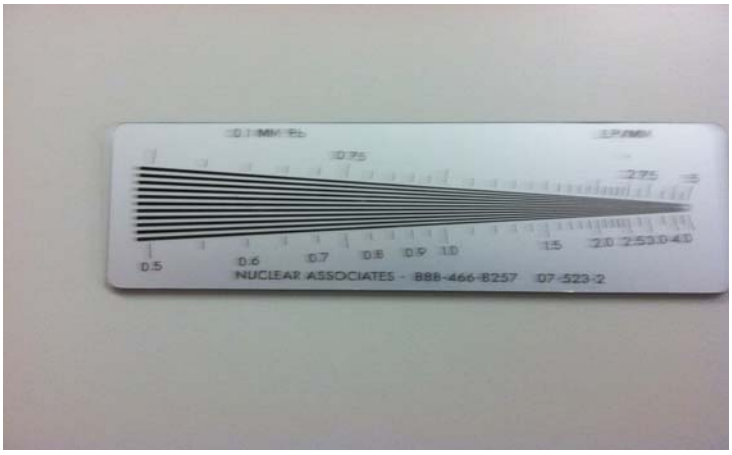

Figure 3.2. The Nuclear Associates spatial resolution tool/Phantom.

The AAPM recommended spatial resolution limits are shown in table 3.1

Acceptable High-Contrast/Spatial Resolution

Image Size (cm)	lp/mm	Image Size (cm)	lp/mm	Image Size (cm)	lp/mm
10	3.33	20	1.66	30	1.11
12	2.77	22	1.51	32	1.04
14	2.38	24	1.39	34	0.98
16	2.08	26	1.28	36	0.92
18	1.85	28	1.19	38	0.88

Table 3.1**.** AAPM Report # 74 Recommended Spatial Resolution Limits.

These resolution limits were used during the collection of spatial resolution data for both II and FPD fluoroscopy units.

3.3 Low Contrast Resolution.

Contrast resolution is determined by viewing a phantom containing various objects that span a range of subtle contrasts. A Westmead Hospital Phantom was used to determine the low contrast resolution capabilities of the radiology equipment in this exercise. This phantom consist of metal blocks or plates with holes of different depths bored into them. With the calibration information, the absolute contrast resolution can be determined using an acrylic thickness of 8” to attenuate the radiation beam and simulate a patient, and take into account the effects of scatter radiation on image acceptability. The phantom is placed on top of the stack of acrylic plates to decrease the magnification of the phantom as seen on the image monitor. A fluoroscopic system in good repair should resolve discs at a contrast level of 3% (the 11^{th} disk in the Westmead phantom). The Westmead low contrast resolution tool/phantom is shown in

figure 3.3 and the low contrast testing setup is shown in figure 3.4. As stated in the previous section, little ambient light was used to score the resolution of each fluoroscopic unit. There was more distance between the observer and the image monitor to help focus on the entire image of the Westmead phantom. Table 3.2 list the recommended low contrast limits set forth by the manufacturer of the Westmead phantom and were used during the scoring of both II and FPD fluoroscopy units.

Acceptable Low Contrast Percent Resolution

Disk Number	%	Disk Number	%	Disk Number	%
7	5	10	3.5	13	1.5
8	4.5	11	3	14	1
9	4	12	2	15	0.5

Table 3.2. Westmead Phantom Recommended Low Contrast Resolution Limits

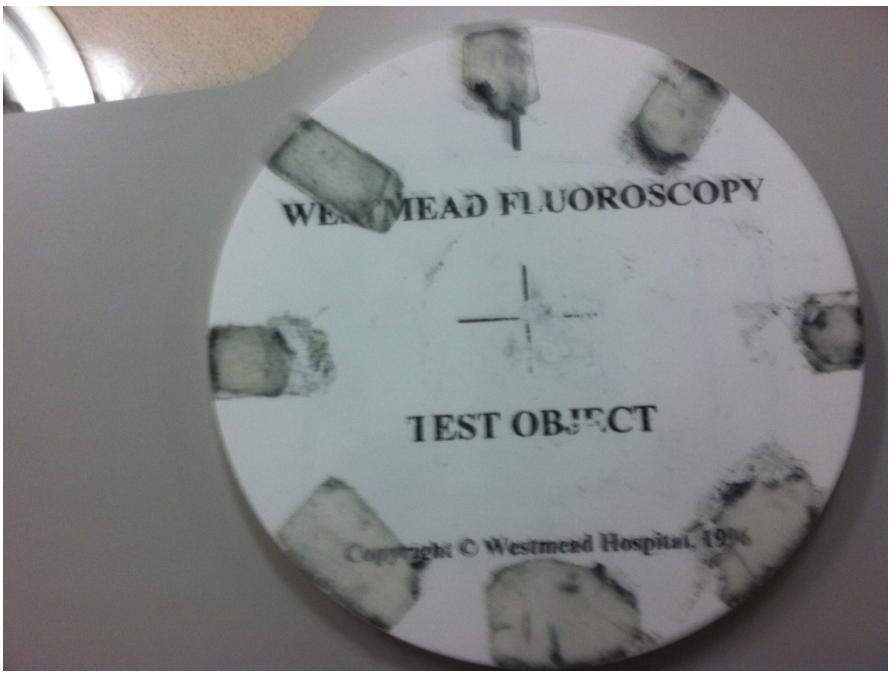

Figure 3.3. The Westmead Low Contrast resolution tool/Phantom.

Figure 3.4. The Westmead Low Contrast resolution tool/Phantom in experimental setup with 8 1’ Acrylic plates.

3.4 Radiation Meter Used

A RTI Barracuda radiation meter was used in this exercise and is shown in figure 3.4.

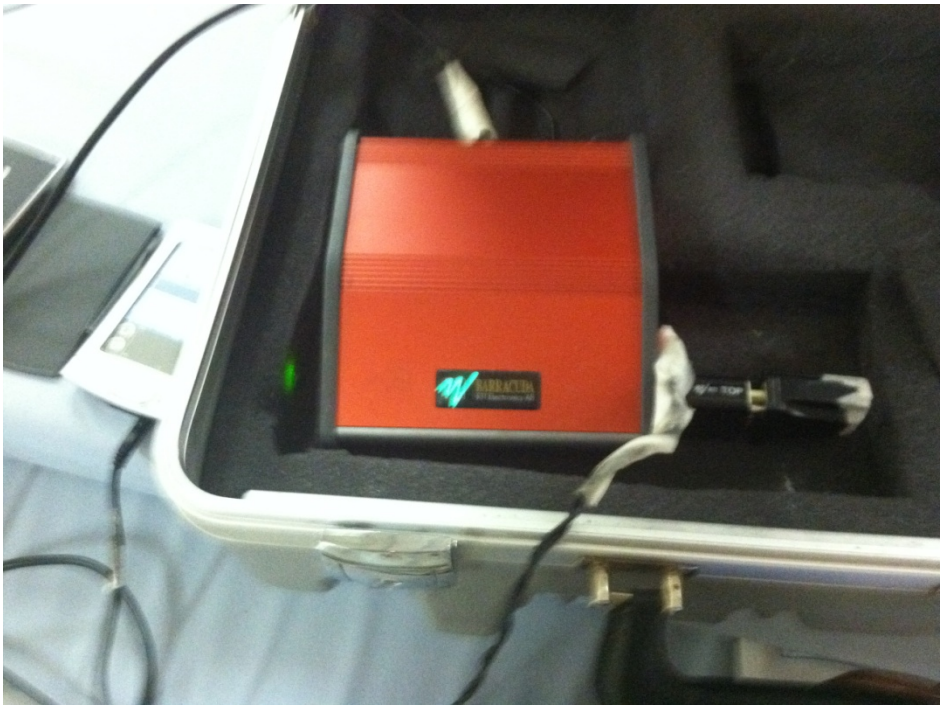

Figure 3.5. The RTI Barracuda “Multi-meter” Radiation Meter.

The Barracuda is an "all-in-one" X-ray multi-meter and is used for quality assurance purposes. The Barracuda can be configured to meet specific needs and requirements. It can measure on all modalities; radiography, mammography, fluoroscopy, pulsed fluoroscopy, dental, panoramic dental and CT systems. The R100 detector probe was used to measure the patient EER in the exercise. This is a dedicated detector for the Barracuda system Radiation Detector: This is a solid state detector and was used to measure the patient EER. Solid state radiation detectors are detectors that use semiconductors as the active material in the detector with electron/hole pairs being created in the semiconductor material. The R100 probe uses a silicon diode semiconductor to quantify the ionizing radiation event. This detector relies on the

photoelectric effect ionization event of the material by the x-ray photon to create an electronic signal that is sent to the meter's microprocessor for processing and displaying the results. This detector/multi-meter combination can be used to measure the following parameters: dose, dose rate, dose/pulse, pulse rate[18]. The range of values of each parameter measured along with the corresponding inaccuracy is listed below in table 3.3.

Measurable Fluoroscopy Parameters

Range	Inaccuracy
Pulse 1 – 65535	±1 pulse
Dose: 30 nGy – 1000 Gy	±5 %
Dose/Pulse Rate: 15 nGy/s – 450 mGy/s	±5 % or ±7 nGy/s
Dose Rate: 0.1 mR/min – 3000 R/min	±5 % or ±0.05 mR/min

Table 3.3. The measurements allowed and corresponding accuracy for the R100/Barracuda Probe Configuration[18].

3.5 Cardiovascular Units Inspected

The three most common manufactures of CVL fluoroscopic imaging equipment were used in this exercise. This was done because of the wide variety of both II and FPD imaging systems that were available, and include Siemens, Philips and Toshiba. The typical fluoroscopic input diagonal sizes ranged from 27 to 10 cm in a typical CVL

suite. A total of 70 units were evaluated for this exercise, with 13 units having an II imaging chain, and the rest having a FPD imaging system. The FPD fluoroscopic unit were tested twice, once in normal dose mode and once in low dose mode and in fluoroscopic and cine imaging mode. The II based fluoroscopy units that were tested, were units that were the latest models available just before FPD units were released to the public. This was done to be sure that the results were not shifted by sub-optimal II based fluoroscopic units.

CHAPTER 4

RESULTS AND DISCUSSION

4.1 Fluoroscopy Mode Imaging

Each unit was categorized by the size of the input detector's diagonal length and the type of input device (II vs. FPD) and mode of operation. With several different units, the data under investigation was averaged for each detector size and plotted comparing the two detector systems under study.

With respect to figure 4.1 shown below, Both II and FPD systems exceeded the recommended spatial resolution limits set by the AAPM in report 74[16]. The average spatial resolution capabilities for 23 to 27 cm and 18 to 22 cm diagonal detectors are shown in table 4.1 as well.

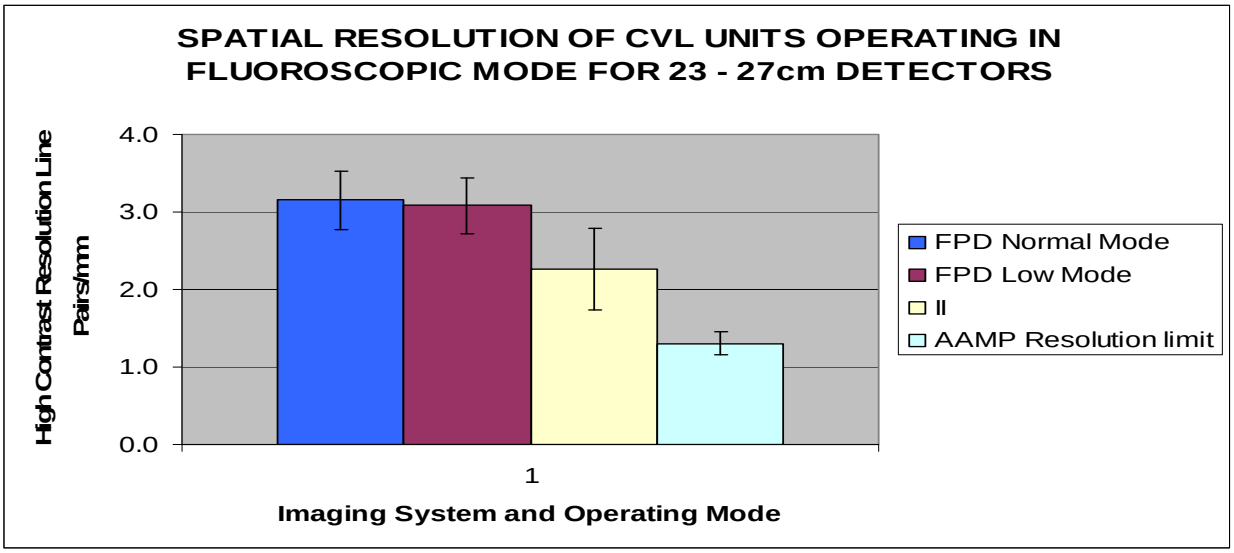

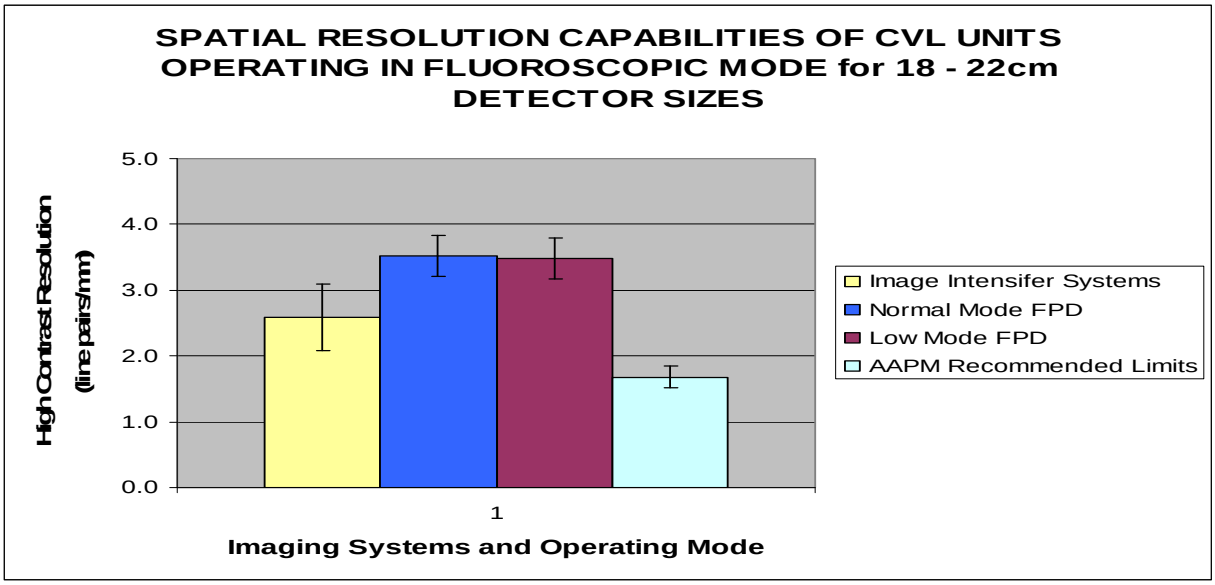

Figure 4.1. Fluoroscopic Mode Spatial Resolution Comparing II and FPD Systems with AAPM Recommended Limits.

Detector Diagonal Size: 23 – 27cm

II	FPD NORM	FPD LOW	AAPM RECOMMENDED
2.3 +/- 0.53	3.1 +/- 0.36	3.1 +/- 0.36	1.3 +/- 0.15

Detector Diagonal Size: 18 – 22cm

II	FPD NORM	FPD LOW	AAPM RECOMMENDED
2.6 +/- 0.54	3.5 +/- 0.32	3.5 +/- 0.32	1.68 +/- 0.17

Table 4.1 Average Spatial Resolution of CVL Imaging Units Operating Fluoroscopy Mode. Units are line pairs/mm.

All units tested in this exercise exceeded the AAPM's recommended spatial resolution limits. This is what was expected because the units have undergone

preventive maintenance and are operating well within each manufacturer's recommended operating standards. In all cases the FPD based systems operating in normal and low dose mode exceeded the II based systems which is related to the higher DQE values for the FPD systems. The uncertainty seen in the resolution data is due to the combined FoV's used in this exercise and latitude used when scoring the resolution tools. Please recall in section two the researched information showed that the FPD systems should be similar in spatial resolution capabilities as compared to the II based systems using low exposure rate dose acquisition modes such as fluoroscopy. The variation of the results discovered in the research reported could be from the increased dose efficiency of newer FPD imaging units and the volume of units tested. Table 4.2 list the percent difference of each imaging system with respect to the AAPM recommended spatial resolution limits.

Detector Diagonal Size: 23 – 27 cm

II	FPD NORM	FPD LOW
54.1	82.4	81.4

Detector Diagonal Size: 18 – 22 cm

II	FPD NORM	FPD LOW
42.6	70.7	69.8

Table 4.2 Percent Difference in Spatial Resolution From the AAPM Recommended Resolution Limits.

There is over an 80% difference in spatial resolution over the recommended limits set by the AAPM when using FPD imaging systems for 23 – 27 cm sized detectors and about 70% difference for 18 – 23 cm sized detectors. When comparing the spatial resolution limits of FPD to II detectors, the percent increase in spatial resolution is over 50% for 23 – 27 cm sized detectors and about 65% difference for 18 – 23cm sized detectors and is shown in table 4.3

Detector Diagonal Size: 23 – 27 cm

II	FPD NORM	FPD LOW
0	52.3	50.4

Detector Diagonal Size: 18 – 22 cm

II	FPD NORM	FPD LOW
0	66.1	64.0

Table 4.3 Percent Increase in Spatial Resolution of FPD Using Normal and Low Dose Mode As Compared to II Systems.

The percent decrease in spatial resolution when comparing FPD in normal to low dose mode, is about 1.3%. This decrease in the spatial resolution is very small and [would not be able to visualize] when imaging the spatial resolution phantom.

Referencing figures 4.1 and table 4.1, based only on those results and the patient EER which will be discussed later, patient exposure to radiation could be reduced and the imaging physician gain an appreciable amount of spatial resolution by imaging with a FPD based system. With respect to figure 4.1 shown above, both the normal and low dose mode in the FPD systems are reasonably comparable in their

spatial resolution capabilities. Again, referencing figure 4.1, and based only on the results of the patient EER which will be discussed later, patient exposure to radiation could be reduced and the imaging physician not suffer any appreciable lost of spatial resolution by considering the use of low dose mode.

With respect to figure 4.2 shown below, Both II and FPD systems meet the recommended low contrast resolution limits set by the AAPM in report 74[19]. The average spatial resolution capabilities for 23 to 27cm and 18 to 22 cm diagonal detectors are shown in table 4.4 as well. Again, this is what was expected because the units have undergone preventive maintenance and are operating well within each manufactures recommended operating standards. No “liberty” was taken here because of the viewing quantification of different individuals when viewing the difference of 1% contrast between adjacent contrast disks and what is actually meant by visualizing a contrast disk. For example, the entire border circumference of the disk should be visualized to score the actual contrast difference of an imaging system.

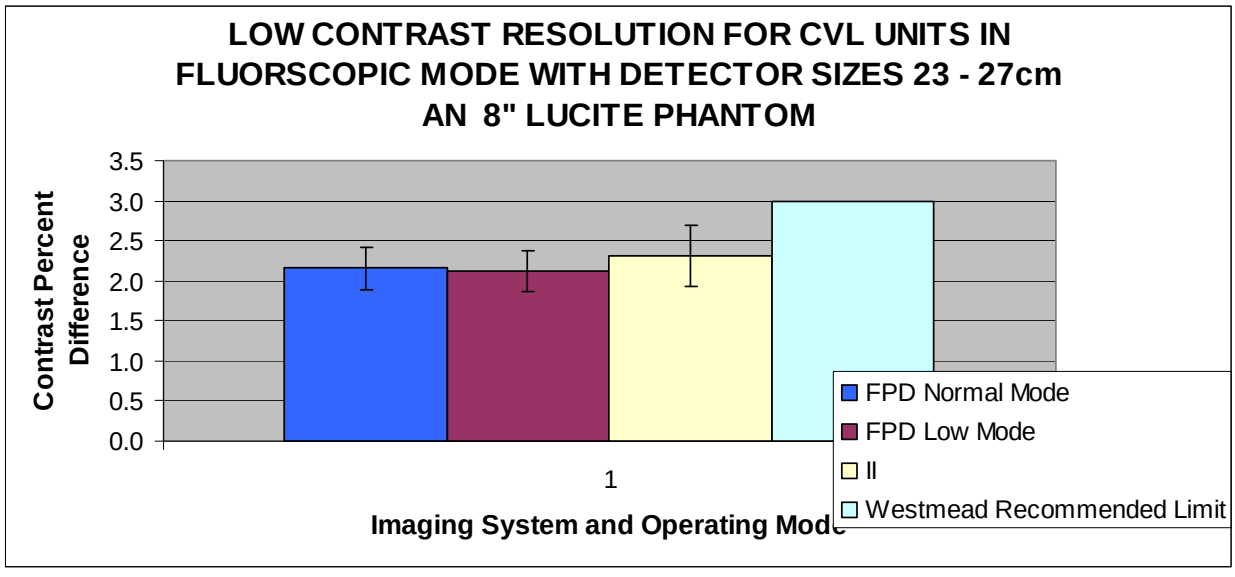

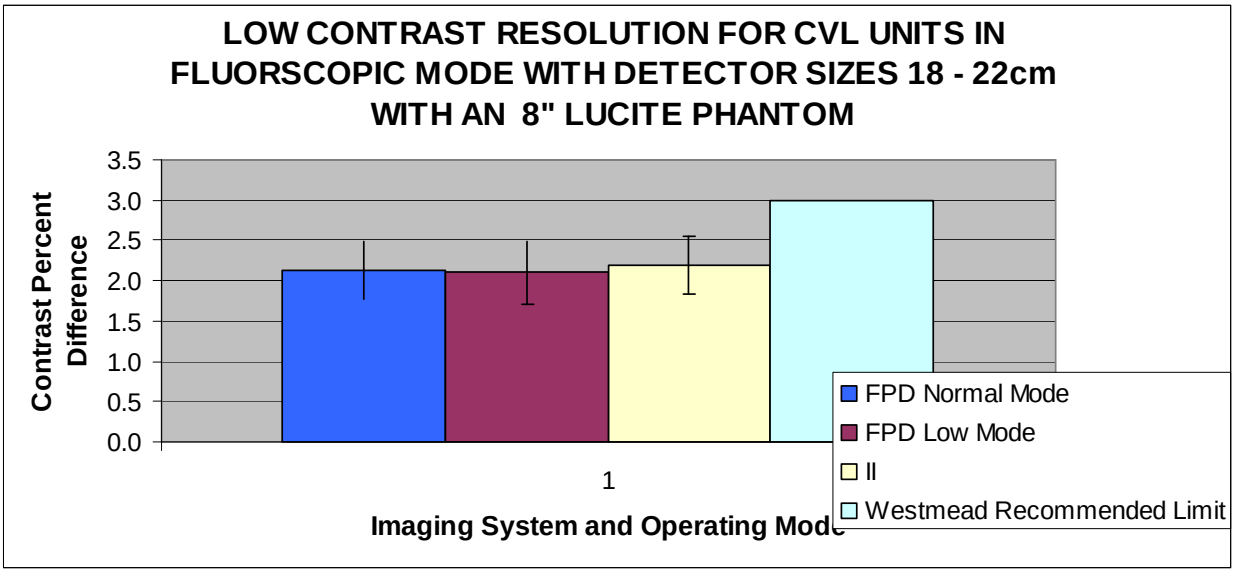

Figure 4.2. Fluoroscopic Mode Low Contrast Resolution Comparing II and FPD Systems to Westmead Phantom Recommend Limits.

Detector Diagonal Size: 23 – 27 cm

II	FPD NORM	FPD LOW	WESTMEAD RECOMMEND LIMIT
2.3 +/- 0.38	2.2% +/- 0.24	2.1% +/- 0.29	3

Detector Diagonal Size: 18 – 22 cm

II	FPD NORM	FPD LOW	WESTMEAD RECOMMEND LIMIT
2.2 +/- 0.36	2.1 +/- 0.35	2.1 +/- 0.39	3

Table 4.4 Average Percent Low Contrast Resolution of CVL Imaging Units Operating Fluoroscopy Mode. Units are percent contrast difference.

Below, table 4.5 list the percent difference of each imaging system with respect to the AAPM recommended spatial resolution limits.

Detector Diagonal Size: 23 – 27 cm

II	FPD NORM	FPD LOW
25.7	32.7	34.1

Detector Diagonal Size: 18 – 22 cm

II	FPD NORM	FPD LOW
31.2	33.8	35.1

Table 4.5 Percent Difference in Low Contrast Resolution from AAPM Recommended Resolution Limits.

There is just over 33% difference in low contrast resolution over the recommended limits set by the Westmead Phantom manufacturer when using FPD imaging systems with 23 – 27 cm sized detectors and about a 34% difference for 18 – 23cm sized detectors. When comparing the low contrast resolution limits of FPD to II detectors, the percent increase in low contrast resolution is about 7% for 23 – 27cm sized detectors operating in normal fluoroscopic mode and 8% while imaging in low dose fluoroscopic mode. There is a 3 percent increase in low contrast resolution for 18 – 22 cm sized FPD detectors over II detector imaging systems operating in normal fluoroscopic mode and a 4% while imaging in low dose fluoroscopic mode (shown in table 4.6).

Detector Diagonal Size: 23 – 27 cm Imaging Systems

II	FPD NORM	FPD LOW
0	6.9%.	8.2%

Detector Diagonal Size: 18 – 22 cm

II	FPD NORM	FPD LOW
0	2.6%	4.0%

Table 4.6 Percent Increase in Low Contrast Resolution of FPD Using Normal and Low Fluoroscopic Dose Mode As Compared to II Systems.

One reason that the FPD-based systems excelled in the low contrast resolution capabilities compared to the II based systems is due to the II's increased noise contributions. Recall in section 2.1, the sequence of events during image formation using an II detector. The signal is converted from x-rays to light photons to electrons back to light photons and then back to electrons when using a CCD imaging camera. This signal conversion adds noise at each change. The percent increase in low contrast resolution when comparing FPD in normal to low dose mode, is about 1.4% for both size ranges. This increase in the low contrast resolution is very small and would not be able to visualize when imaging the low contrast resolution phantom.

Referencing figure 4.2, based only on the results and the patient EER (which will be discussed later), patient exposure to radiation could be reduced and the imaging physician would gain just a small amount of low contrast resolution by imaging with a FPD based system. With respect to figure 4.2 shown above, both the normal and low dose modes in the FPD systems are reasonably comparable in their low contrast

resolution capabilities. Again, referencing figure 4.2 and based only on the results of the patient EER (which will be discussed later), patient exposure to radiation would be reduced and the imaging physician maintains the relative same low contrast resolution by the use of low dose mode.

With respect to figure 4.3 and table 4.7 and 4.8, shown below, the FPD detectors operating in normal fluoroscopic mode have a slightly lower EER as compared to II imaging systems. This is what is expected when considering that the DQE was similar as stated in section number 2 of this report. While there is a moderate percent decrease in the EER of about 10% between the FPD systems and the II systems operating in normal fluoroscopic mode, there is a significant percent difference when comparing II imaging systems and low dose FPD imaging systems. This percent difference is shown in table 4.8 for both detector size ranges. For the larger 23 to 27 cm size, the percent difference is about 57%. The biggest difference in the EER occurs when the FPD imaging systems are operated in low dose mode, the smaller 18 to 22 cm size detectors showed a percent decrease of about 81%.

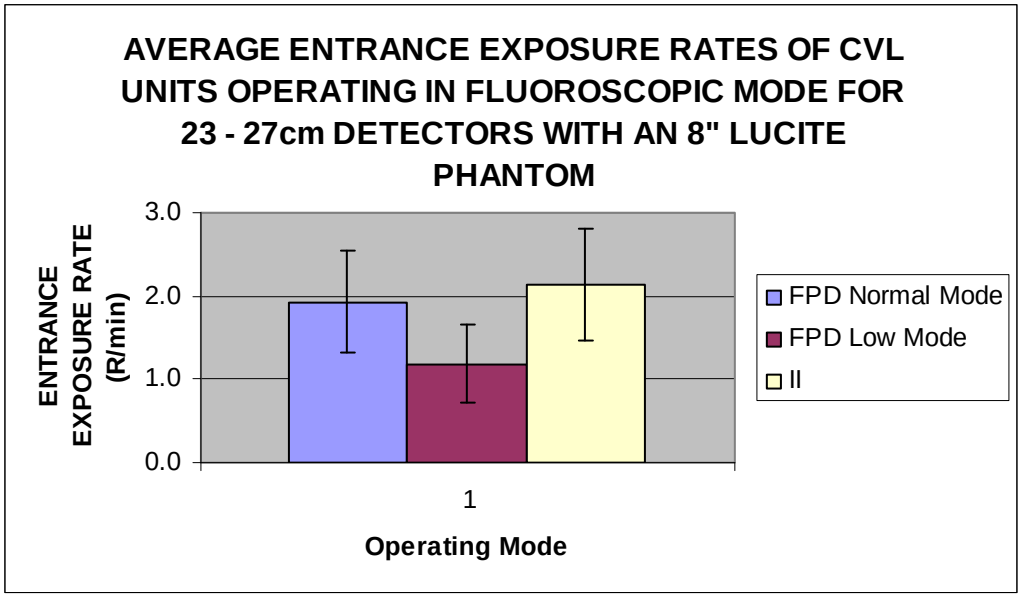

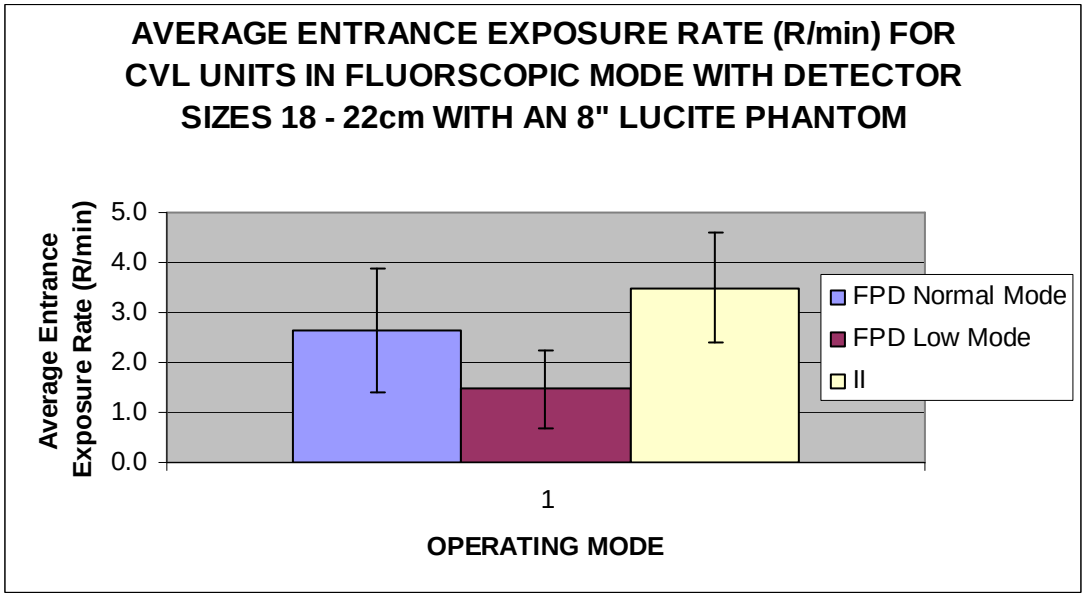

Figure 4.3. Fluoroscopic Entrance Exposure Rates Comparing the II System to FPD Systems Operating in Normal and Low Operating Modes

Detector Diagonal Size: 23 – 27 cm

II	FPD NORM	FPD LOW
2.1mR/min +/- 0.68	1.9mR/min +/- 0.62	1.2mR/min +/- 0.46

Detector Diagonal Size: 18 – 22 cm

II	FPD NORM	FPD LOW
3.5mR/min +/- 1.1	2.6mR/min +/- 1.2	1.5mR/min +/- 0.78

Table 4.7 Average EER of CVL Imaging Units Operating in Fluoroscopy Mode.

Detector Diagonal Size: 23 – 27 cm

II	FPD NORM	FPD LOW
0	10.2%	57.6%

Detector Diagonal Size: 18 – 22 cm

II	FPD NORM	FPD LOW
0	27.8%	81.4%

Table 4.8 Percent Difference of the Average EER of CVL Imaging Units Operating in Fluoroscopy Mode.

These large differences are thanks in large part to the ability to remove image noise during the image reconstruction process by using special noise reducing algorithms, the real dose saving occurs when the FPD systems are operated in the low dose mode. With reference to Table 4.9 below, the percent decrease in the EER ranges from 38 to 44 percent

comparing low dose to normal dose mode for 23 to 27cm and 18 to 22cm diagonal FPD imaging systems respectfully.

Detector Diagonal Distance: 23 – 27 cm

FPD NORM	FPD LOW
0	38.8%

Detector Diagonal Distance: 18 – 22 cm

FPD NORM	FPD LOW
0	44.2%

Table 4.9 Percent Difference of the Average EER of FPD CVL Imaging Units Operating in Fluoroscopy Mode.

As a extra additional benefit, when the patient EER is reduced, the amount of scatter radiation that the operator and surrounding individuals receive will be decreased as well because of the decreased x-ray photon concentration in the radiation beam when compared to II based imaging systems. The scatter exposure rate can be further reduced by considering the use of the low dose mode for the same reason explained above. The uncertainty seen in the EER is due to a few factors: 1) The reproducibility of exposure of the radiation detector alone is +/- 5% mR. 2) The reproducibility of exposure of the imaging unit is +/- 4.5% and is due to the fluctuations of the exposure parameters (kVp, mA and exposure pulse length).

4.2 Cine Mode Imaging

The results of image quality testing under cine imaging are detailed in this section. As expected, the FPD systems showed superior image quality in both the spatial and low resolution over II imaging systems as can be seen in figure 4.4 and figure 4.5 seen below.

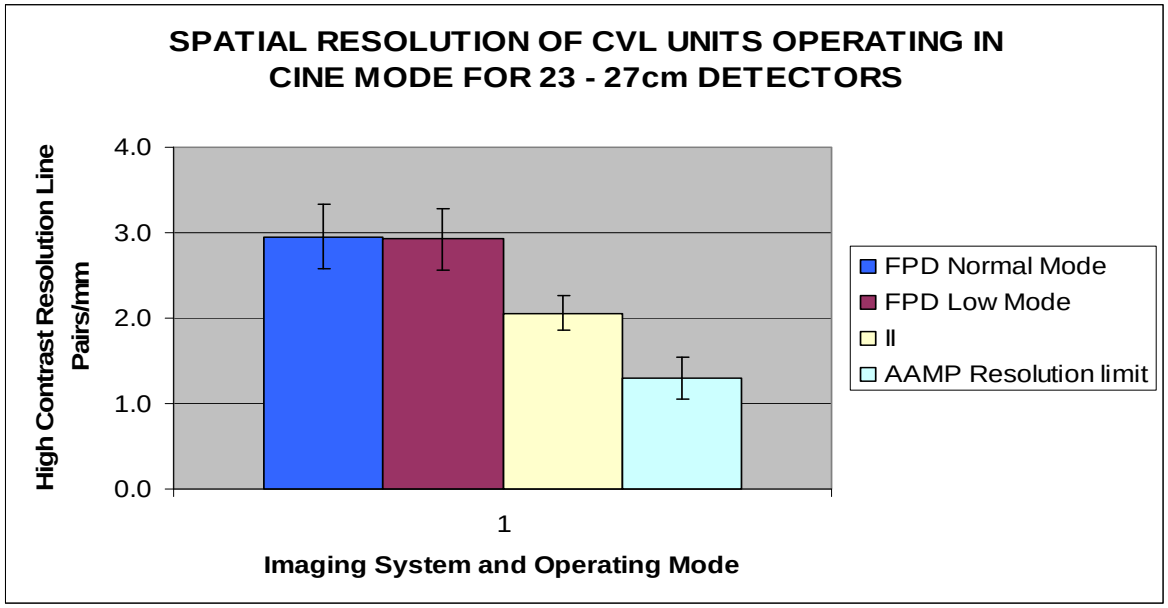

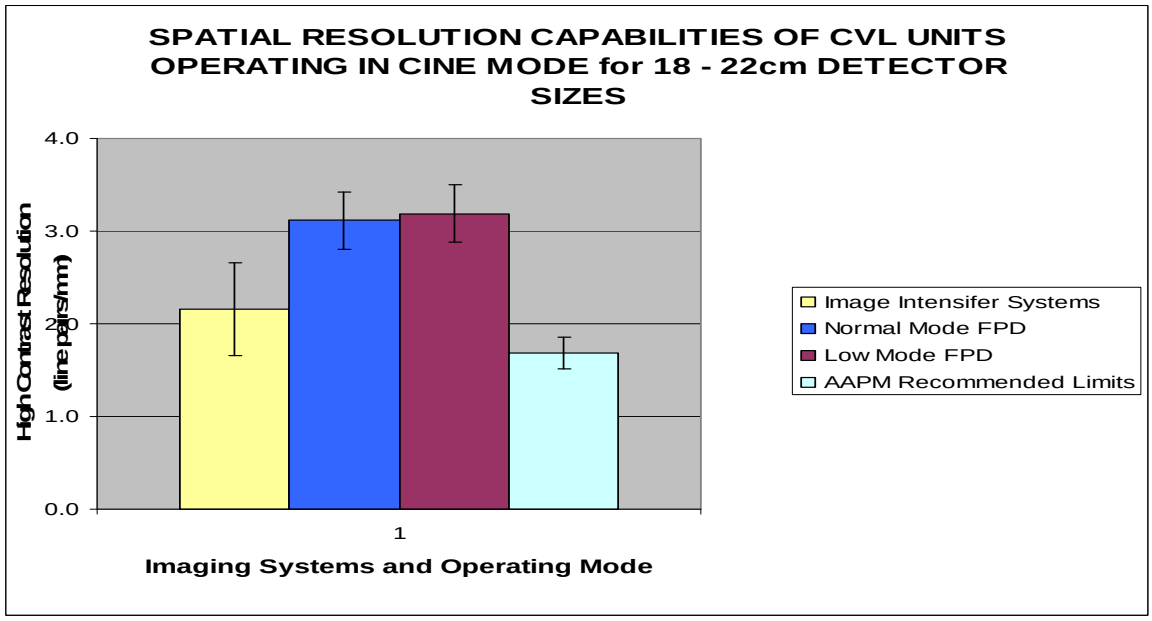

Figure 4.4. Cine Mode Spatial Resolution Comparing II and FPD Systems with AAPM Recommended Limits.

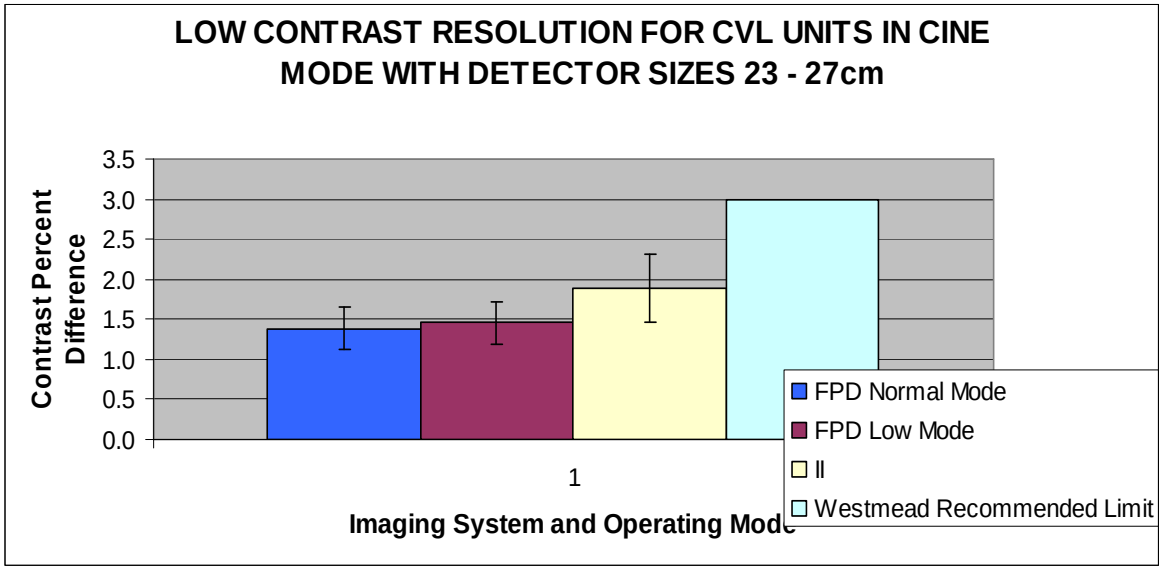

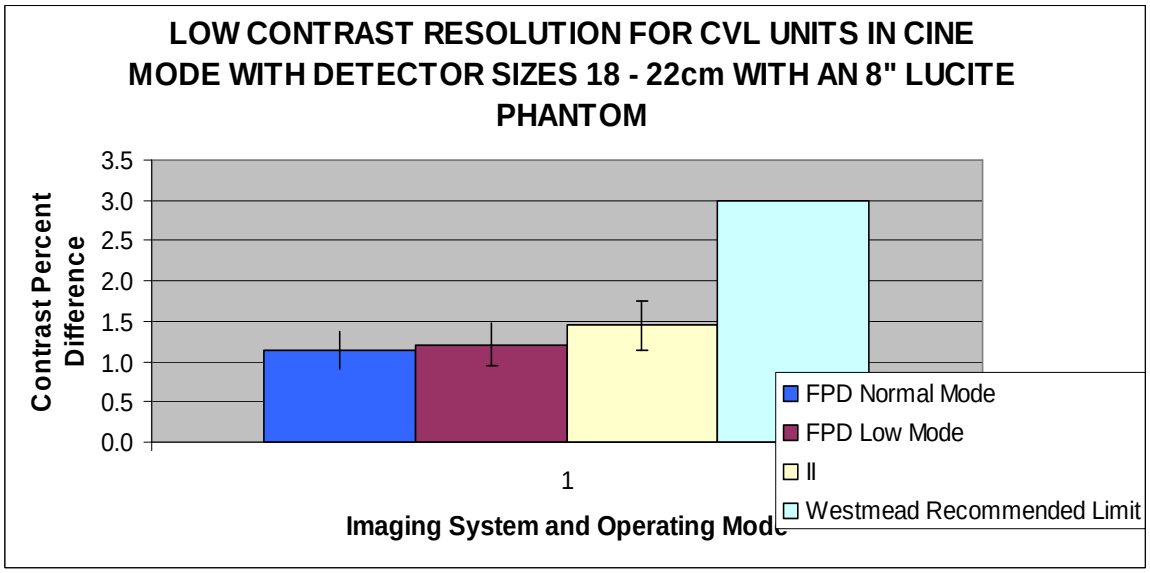

Figure 4.5. Cine Mode Low Contrast Resolution Comparing II and FPD Systems to Westmead Phantom Recommend Limits.

Table 4.10 below, details the spatial resolution capabilities of CVL units operating in cine mode. As expected, both FPD and II imaging systems exceeded the resolution limits set by the AAPM.

Detector Diagonal Size: 23 – 27 cm

II	FPD NORM	FPD LOW	AAPM RECOMMENDED
2.1 +/- 0.19	3.0 +/- 0.50	2.9 +/- 0.69	1.3 +/- 0.15

Detector Diagonal Size: 18 – 22 cm

II	FPD NORM	FPD LOW	AAPM RECOMMENDED
2.2 +/- 0.29	3.1 +/- 0.34	3.2 +/- 0.53	1.68 +/- 0.17

Table 4.10. The Average Spatial Resolution of CVL Imaging Units Operating in Cine Mode. Units are line pairs/mm.

With respect to figure 4.4 and figure 4.1, one will notice that the spatial resolution for both the FPD and II systems was degraded when comparing the cine mode spatial resolution to the fluoroscopic mode spatial resolution. For the cause of this concern, please recall that in section 2 it was mentioned that the bandwidth (the speed of the electronic readout) affects the resolution. The individual cine recorded images have to be able to stand alone and display an image quality that makes clinical diagnosis possible. For this image quality to exist, the cine digital signal will contain a much larger amount of information in the form of digital bytes than the digital signal transmitted during fluoroscopy image. The bandwidth can only handle a certain amount of information before the video system has to make concessions to keep the image viewing and recording process in progress. The viewing system does this by

compressing the signal's information by interpolating the signal, which causes the signal to lose some of its sharp shape and results in a decrease of spatial resolution. The percent difference decrease in spatial resolution is shown in the table 4.11 below.

Detector Diagonal Distance: 23 – 27 cm

II	FPD NORM	FPD LOW
9.1	6.5	6.7

Detector Diagonal Distance: 18 – 22 cm

II	FPD NORM	FPD LOW
16.7	12.1	9

Table 4.11, The Percent Decrease in Spatial Resolution of CVL Imaging Units Operating Cine Mode as compared to Fluoroscopic Mode.

To keep from getting deluged with information please note that while operating in cine imaging mode, the FPD imaging systems excelled in their ability to provide an image with both spatial and low contrast resolution. With this in mind, the dialogue will shift to the decrease in the phantom's measured EER that the FPD systems allowed as compared to II systems.

With respect to figure 4.6 below, the phantom's EER is decreased by imaging with a FPD system as compared to an II imaging system. The percent decrease in the EER is comparable to the decrease seen while imaging in the fluoroscopic mode.

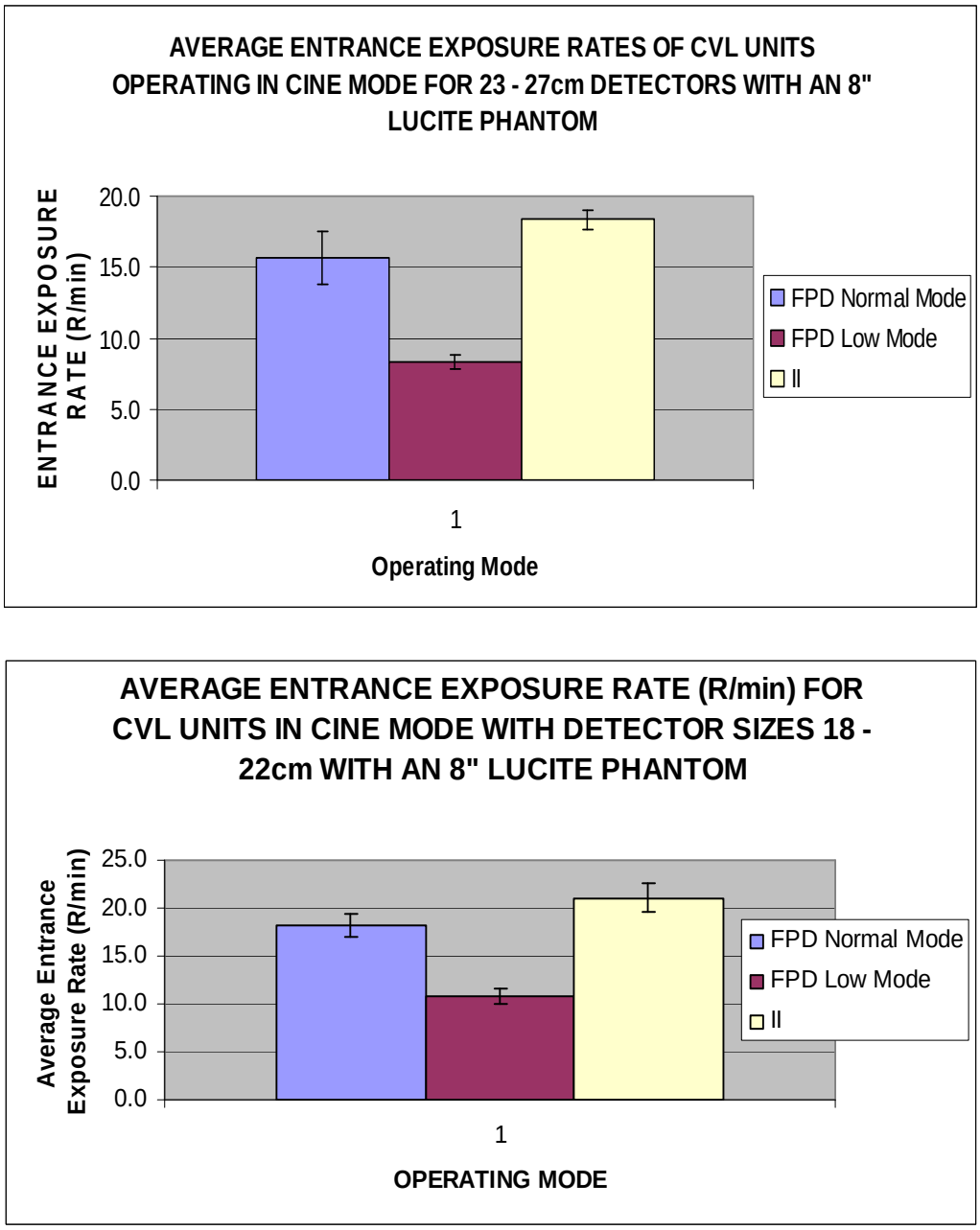

Figure 4.6. Cine Entrance Exposure Rates Comparing the II System to FPD Systems Operating in Normal and Low Operating Modes

Detector Diagonal Size: 23 – 27 cm

II	FPD NORM	FPD LOW
18.4mR/min +/- 0.83	15.6mR/min +/- 1.83	8.2mR/min +/- 1.49

Detector Diagonal Distance: 18 – 22 cm

II	FPD NORM	FPD LOW
21.1mR/min +/- 1.54	18.2mR/min +/- 1.91	10.9mR/min +/- 1.87

Table 4.12 Average EER of CVL Imaging Units Operating in Cine Mode.

With reference to table 4.13 shown below, a lowering of the phantom's EER can be achieved by using a FPD imaging system and significantly lowered by operating in the FPD system in the low dose mode.

Detector Diagonal Size: 23 – 27 cm

II	FPD NORM	FPD LOW
0	16.6%	76.4%

Detector Diagonal Size: 18 – 22 cm

II	FPD NORM	FPD LOW
0	14.5%	68.8%

Table 4.13 Percent Difference of the Average EER of CVL Imaging Units Operating Cine Mode.

With reference to table 4.14, the percent decrease in the phantom's EER is reduced by around 40 to 47% by operating the FPD in the low dose mode. This is a significant dose lowering by just selecting the low dose mode.

Detector Diagonal Size: 23 – 27 cm

FPD NORM	FPD LOW
0	47.2%

Detector Diagonal Size: 18 – 22 cm

FPD NORM	FPD LOW
0	40.2%

Table 4.14 Percent Difference of the Average EER of CVL Imaging Units Operating in Cine Mode.

The raw data that was collected in this exercise is listed in the appendix.

CHAPTER 5

CONCLUSION

One very important truth remains: exposure dose and image resolution mean nothing when they are not compared together. The lowest dose to the patient means nothing if the operator cannot have a clinically acceptable image to guide them during a fluoroscopic procedure.

It should be realized that some patient body sizes will not allow the use of a low mode and still allow for clinically acceptable images. With this in mind, it should be easier to increase the dose rate when needed than to decrease the dose rate when not needed. It has been seen that a majority of imaging facilities the author of this exercise consults with will have the default setting at a normal dose rate. The facilities will change the default setting when shown that the dose saving will not adversely affect the imaging resolution capabilities.

By moving to the modern FPD imaging systems patient and operator exposure can be reduced compared to II based systems. With this switch, a reduction in the EER is about 10%. When possible the operator of the imaging system should consider the option of performing the examination in the low exposure dose mode. This was shown to reduce the EER by 38 to 47.2%. It should also be known that none of the imaging systems tested in this exercise displayed any imaging artifacts that were discussed in section number 2.

As the advent of better computing and integrated circuits systems, the patient exposure rate is sure to decrease. One area of promise is the development of the solid-

state x-ray image intensifier (SSXII)[19]. This device shows promising results of better spatial resolution and exposure reduction.

REFERENCES

1. Schueler, Beth, PhD, The AAPM/RSNA Physics Tutorial for Residents: General Overview of Fluoroscopic Imaging, Radiographics, Volume 20, Issue 4, July 2000

2. Sprawls, Perry, Ph.D. The Physical Principles of Medical Imaging, Sprawls Educational Foundation, Open Resources for Learning and Teaching. http://www.sprawls.org

3. Bushong, Stewart, Sc.D, Radiologic Science for Technologists, 5th Edition, copyright 1993, page 147.

4. Copyright © Sparks in Physics Web Site

5. Wikibooks, Basic Physics of Digital Radiography/The Patient

6. Sivananthan,M.U., Moore, J., Cowan, J.C., Pepper, C.B., Hunter, S., A Flat-Detector Cath Lab System in Clinical Practice, Philips Healthcare

7. Wang, Jihong, PhD,. Blackburn, Timothy J, PhD, The AAPM/RSNA Physics Tutorial for Residents X-ray Image Intensifiers for Fluoroscopy

8. J. Seibert, Anthony, 2006 Flat-panel detectors: how much better are they? Pediatric Radiology. 2006 September; 36(Suppl 2): 173–181.

REFERENCES (Continued)

9. Nickoloff, Edward Lee, DSc, AAPM/RSNA Physics Tutorial for Residents: Physics of Flat- Panel Fluoroscopy Systems, Radiographics, Volume 31, Number 2 ,RSNA 2011

10. Geisler, William R., M.S. DABR Department of Radiology/Medical Physics Fluoroscopy in Specials: Flat Detector vs. Image Intensification

11. Dr Jeremy Jones and Stefano Pacifici, Detective Quantum Efficiency, http://radiopaedia.org/articles/detective-quantum-efficiency-1

12. Padovani, R. S., Della, Maria, Misericordia Hospital, Basic Principle of Flat Panel Imaging Detectors. 2006

13. INTERNATIONAL ATOMIC ENERGY AGENCY, Diagnostic Radiology Physics A Handbook for Teachers and Students Vienna, September 2014

14. Anderson, Charles M. MD, PhD, Leidholdt, Edwin M, Jr. PhD, An Introduction to Fluoroscopy Safety, Version: August 19, 2013

REFERENCES (Continued)

15. Mahadevappa, Mahesh, PhD Imaging & Therapeutic Technology Fluoroscopy: Patient Radiation Exposure Issues Volume 21, Issue 4 July 2001, RSNA 2001

16. Lin, PP, Acceptance testing of automatic exposure control systems and automatic brightness stabilized fluoroscopic equipment, in Quality Assurance in Diagnostic Radiology, AAPM Monograph No. 4, 1980

17. AAPM REPORT NO. 74, Quality Control In Diagnostic Radiology stay

18. www.rti.se/products/barracuda

19. Kuhls-Gilcrist, Andrew, Yadava, Girijesh, Patel, Vikas, Amit Jain, Bednarek, Daniel R., and Rudin, Stephen The Solid-State X-Ray Image Intensifier (SSXII): An EMCCD-Based X-Ray Detector

APPENDIX A

ENTRANCE EXPOSURE RATE of CVL UNITS
FLUORO 23 - 27cm

II	FPD NORM	FPD LOW
3.4	2.4	2.4
1.9	2.3	1.1
1.5	2.21	1.76
1.45	1.45	0.9
1.93	1.9	1.5
3.45	2.2	1.2
1.75	0.9	0.74
2.25	1.43	0.95
1.9	1	0.8
1.85	2.1	1.5
2.15	2.2	1.37
	1.2	0.52
	1.8	0.91
	3.3	1.55
	2.1	0.85
	2.4	1.2
		0.85

APPENDIX B

ENTRANCE EXPOSURE RATE of CVL UNITS
FLUORO Mode Detector Size18 - 22cm

II	FPD NORM	FPD LOW
4.2	4.55	3.9
2.95	4.51	1.61
2.3	0.87	0.5
2.25	2.75	2.45
2.85	4.6	0.66
4.95	1.35	0.55
3.2	1.6	0.87
3.37	3.5	1.4
5		1.2
5	1.73	1.1
2.4	2.4	1.32
	3.83	1.91
	3.7	1.75
	0.94	0.55
	1.33	0.62
	1.8	1.25
	3.1	2
	1.47	1.05
	1.7	1.15
	1.66	1.4
	2.35	2
	2.95	1.63
	3.7	2.15
	3.9	1.2
	3.13	2.62
		1.2

APPENDIX C

ENTRANCE EXPOSURE RATE of CVL UNITS
Cine Mode Detector Size 23 - 27cm

II	FPD NORM	FPD LOW
17.7	14.8	8.6
17.4	15.3	9.6
18.8	15.2	7.5
19.1	15.1	5.8
19.2	14.2	7.7
18.1	15.6	7.4
17.8	15.3	8.4
19.3	16	11.1
18.2	16.5	8.1
17.9	17.8	7.9
18.4	17.2	9.6
	13.3	
	11.9	
	15.3	
	19.4	
	18.2	
	14.3	
	17	
	14.5	

APPENDIX D

ENTRANCE EXPOSURE RATE of CVL UNITS
Cine Mode Detector Sizes 18 - 22cm

II	FPD NORM	FPD LOW
23.7	18.2	10.9
22.6	18.2	11.7
21.3	18.2	11.2
21.3	18.7	11.2
20.2	18.7	13.6
19.2	18.4	12.3
19.9	17.9	9.1
18.8	14.8	8.7
19.8	17.4	7.9
21	16.3	9.6
22.5	16.7	13.1
20.4	18.7	12.7
23.1	18.7	13.2
	19.4	8.9
	20.1	9.3
	20.4	9.3
	17.2	9.6
	15.5	
	20.7	
	20.7	
	21.2	
	15.9	
	14.9	
	21.4	
	16.8	
	18.7	
	19.9	
	16.7	

APPENDIX E

High Spatial Resolution of CVL UNITS
Fluoroscopic Mode Detector Size 23 - 27cm

II	FPD NORM	FPD LOW
3.5	3.5	4
2.8	3	2.75
2	3.5	3.5
2.5	3	2.75
3	3.5	3
2	3	3
2	3.5	3.3
2	3.3	2.75
2.5	2.75	3.3
2.3	3	3
2	3	3
	3	2.75
	2.75	2.75
	3.3	3.5
	3.5	3.5
	3	2.75
		3

APPENDIX F

Low Contrast Resolution
Fluoroscopic Mode Detector Size 23 - 27cm

II	FPD NORM	FPD LOW
2	2.5	2.5
2.5	2	2
2	2	2.5
2	2	2
2.5	2	2
2	2	2
1.5	2	2
2	2.5	
2	2.5	2.5
2	2	2
	2	2
	2.5	2.5
	2	2
	2	2
	2.5	2.5
	2	2
		1.5

APPENDIX G

High Spatial Resolution of CVL UNITS
Fluoroscopic Mode Detector Sisz 18 - 22cm

II	FPD NORM	FPD LOW
3.1	3	3
4	3	3
3	3	3
3	3.5	3.5
3.5	4	3.5
2.5		3.5
2.5	3	3
2.5	3.5	3.5
2.75	3.5	3.5
2.5	3.5	3.5
2.75	3.5	3.5
	3.3	3.3
	3.5	3.5
	3.5	3.5
	3.5	3.5
	3.3	3.3
	3.8	3.8
	3.5	3.5
	3.5	3.5
	3.5	3.5
	4	4
	3.5	3.5
	4	4
	4	4
	4	4
		3.5

APPENDIX H

Low Contrast Resolution
Fluoroscopic Mode Detector Size 18 - 22cm

II	FPD NORM	FPD LOW
1.5	2.5	2.5
2	2	2
2	2.5	2.5
2.5	1.5	1.5
2	2.5	2.5
2.5		2.5
1.5	2	2
2.5	2	2
2.5	1.5	1.5
2.5	2.5	2.5
2.5	2	2
	2	2
	2.5	2.5
	2	2
	2.5	2.5
	2	2
	2	2
	2	2
	2.5	2.5
	2.5	2.5
	2.5	2.5
	2	2
	2.5	2.5
	1.5	1.5
	2	2
		1.5

APPENDIX I

High Spatial Resolution of CVL
UNITS
Cine Mode Detector Size 23 - 27cm

II	FPD NORM	FPD LOW
2.2	3	2.75
2	3.3	3.5
2.3	3	3.5
1.8	3.3	1.8
2	3	2.1
2.2	2.5	2.75
2.3	2.75	3.5
1.9	3.5	3.5
1.8	2.75	2.5
2.1	3.5	2.3
2	1.8	2.75
	2.1	
	2.75	
	3.5	
	3.5	
	2.75	
	3.2	
	2.5	
	2.3	

APPENDIX J

Low Contrast Resolution
Cine Mode Detector Size 23 - 27cm

II	FPD NORM	FPD LOW
1.5	1.5	2
1.5	1.5	1.5
1.5	1.5	1.5
2.5	1.5	1
2	1.5	1.5
2	1	1.5
2	2	1.5
2.5	1.5	1.5
1.5	1	1.5
2	1.5	1.5
2	1	1
	1.5	
	1.5	
	1.5	
	1.5	
	1.5	
	1	
	1	
	1.5	

APPENDIX K

High Spatial Resolution of CVL
UNITS
CINE MODE DETECTOR SIZE 18 - 22cm

II	FPD NORM	FPD LOW
2.2	3.2	3.1
2.4	3.3	3
2.2	3	3.5
2.5	3.3	4
2.3	2.8	3
2.4	2.75	3.3
1.9	2.8	3.5
1.8	2.75	3
1.7	2.75	3.5
2.2	3	2
2.1	2.8	2.5
	2.75	2.75
	3	3.5
	3.5	2.75
	3.3	3
	4	3.5
	3	3
	3.3	
	3.5	
	3.5	
	3.5	
	3.5	
	3	
	3	
	2.5	
	3.2	
	2.5	
	2.75	

APPENDIX L

Low Contrast Resolution
CINE MODE DETECTOR SIZE 18 - 22cm

II	FPD NORM	FPD LOW
1	1	1.5
1.5	1	1.5
1.5	1	1
1.5	1.5	1
1.5	1	1.5
1.5	1.5	1.5
1	1	1
1.5	1.5	1
1.5	1.5	1
1.5	1	1
1.5	1	1
	1	1.5
	1	1
	1	1
	1	1
	1	1
	1.5	1.5
	1.5	
	1	
	1	
	1	
	1	
	1	
	1.5	
	1	
	1	
	1	
	1	